University of Nevada

Reno

A Study of the Residence Time Distribution Curves of a Rotary Tubular Reactor for Processing Slimy Ores

A thesis submitted in partial fulfillment of the requirements for the degree of Master of Science in Metallurgical Engineering

by

Margaret Kent Witte III

August 1976

The thesis of Margaret Kent Witte is approved:

James L. Hendrix 8/2/76
Thesis Advisor

Roger W. Smith 8/2/76
Department Chairman

Robert W. Fornell 8/2/76
Dean, Graduate School

University of Nevada

Reno

August 1976

ACKNOWLEDGEMENTS

The author wishes to express her appreciation to Dr. James L. Hendrix for his help and guidance throughout the entire experimental investigation.

Special thanks go to Dr. Ken Broadhead of the United States Bureau of Mines for his assistance with the naturally occurring radioactive tracers.

Thanks also go to Mr. Craig Kent, Mr. William Witte and Mr. Michael Partridge for their technical and analytical assistance during the experimentation.

The author wishes to thank Mr. Daniel Kappes for his timely suggestions and advice, and she gratefully acknowledges the financial assistance from the National Science Foundation.

ABSTRACT

A rotary tubular reactor was designed and built to study its mixing characteristics for slimy and non-slimy ores. Residence time distribution tests were conducted on the reactor using a slimy and non-slimy tracer. The rotary tubular reactor was modeled by a set of residence time distribution functions, a dispersion model, and by n-number of constant stir tanks in series.

The study showed that the rotary tubular reactor has mixing patterns that possess characteristics of a plug flow reactor and a constant stir tank. The mixing patterns display a large amount of axial dispersion as well as radial dispersion. The slimy ore displays more axial dispersion than the non-slimes.

The rotary tubular reactor was tested against a constant stir tank reactor and a plug flow reactor. The rotary tubular reactor produced results that were ten times better than those results produced by the constant stir tank reactor or plug flow reactor.

TABLE OF CONTENTS

LIST OF ILLUSTRATIONS

Figure Page

Figure | Page

LIST OF TABLES

LIST OF APPENDICES

INTRODUCTION

New types of tubular reactors for chemical and metallurgical processes have been under extensive study in recent years.[2,6] Satisfactory and economical methods of processing must be found so that low-grade and complex ores may be treated.[4] The economic aspect has prompted the study of many of the latest reactors. Reactors previously studied, especially tubular reactors, have generally been proven feasible for one specific process with no general industrial uses discussed. Most research has been done with models of tubular reactors that exhibit plug flow kinetics.

Baffled tubular reactors have been studied to a lesser extent. To the author's knowledge there has been only one case reported in the literature of a baffled rotating tubular reactor. A baffled rotating tubular reactor was studied by Jennings, et al.,[12] for the precipitation of cuprous telluride by contacting a tellurium-rich solution with copper shot. In this particular case, the system had one continuous phase and one batch phase (i.e. only liquid flowed through the reactor with the copper shot being retained in the reactor). Thus, the data obtained are not applicable to a continuous two phase system (i.e. solution and ore flowing through the reactor).

A rotating mixer reactor has been studied.[2] This reactor is based on a ball mill design, which mixes solid

and gas particles by rotation. Again the reactor was run as only a one phase continuous system with the gas flowing through the reactor and the solids being retained within the reactor. The study was also carried out with the reactor at high temperatures and the rotating mixer reactor is an alternative method to fluidized bed systems.

Many unbaffled tumblers have been studied along with an array of tube digesters and non-rotating forms of tubular reactors. Models of such reactors have been studied by Bielfeldt,[6] McKinstry,[16] Anderson[1] and Dittman.[11] After reviewing the literature it was found that all of the previous reactor systems were not applicable to evaluating a baffled rotary tubular reactor as a primary reaction vessel because the leaching is a two phase continuous system.

This project was initiated to evaluate the effectiveness of a rotary tubular reactor as a hydrometallurgical device for the chemical leaching of slimy ores. Most common slimes containing valuable minerals are in the form of clays. Also, when dealing with the low grade ores, grinding must be done to achieve a great surface area per unit weight of ore. When grinding is accomplished, the slimy characteristics of the ore are enhanced. The finely ground ore approaches the behavior of the clay slimes. The reactors currently used are not satisfactory for effectively processing slimy ores. Leaching in constant stir tanks causes slimes to climb up the sides of the reactor wall or stay on the fluid surface. A plug flow reactor is also unsatisfac-

tory because the slimes become stratified within the reactor and are carried through in segregated flow, unreacted. All other studies on tubular reactors have not used slimy ores as feedstocks. The rotary tubular reactor is an alternative to all current types of commercial reactors. Its mixing characteristics are unlike any of the previously mentioned reactors.

One of the more important parameters of the material flowing through the reactor is the residence time distribution (RTD). The RTD functions define the degree of mixing and the life expectancy of the solid particles in the reactor. Consequently a study of the residence time distribution functions of material flowing through a reactor will give the information necessary to discuss the degree of mixing. Both Levenspiel[14] and Smith[18] define the existing models for most present systems and derive the relationships needed to compare any new reactor design to the existing models.

Research was undertaken to prove that the rotary tubular reactor concept would produce better mixing conditions for handling slimy ores. A baffled rotary tubular reactor was designed and built from plexiglass. Residence time distribution studies were carried out with the reactor, producing a set of RTD curves for both liquid and solid phases. The liquid residence time distribution curves were produced by injecting an inert solution into the system and measuring the intensity of the exit stream

on a spectrophotometer. The solids were followed through the reactor by using a naturally occurring radioactive material and measuring the counts per gram in the exit flow.

The existing ideal models were compared with the experimental curves predicting the mixing performance of the new reactor design. The rotary tubular reactor residence time distribution data were compared with the constant-stir-tanks-in-series modeling data. From this comparison a predictive modeling number was obtained.

Slimes were also tested in the reactor by using a slimy tracer in a similar set of studies. A constant stir tank was then constructed and a plug flow reactor was simulated so that experimental comparisons of the mixing could be made between the reactors. The comparisons of the mixing patterns were made with a sulfuric acid-chalcopyrite leach.

THEORY

An initial step in reactor design is the material balance for the reactor expressed for any reactant or product. The material balance provides the basis for relating the production rate and composition of products to the chemical reaction rate. It is also the basis for deriving the equations needed to define the mixing patterns of a reactor when an inert tracer is present. The general mass balance applicable to any type of reactor is:

$$\left[\begin{array}{l}\text{Mass of reactant}\\ \text{fed to volume}\\ \text{element}\end{array}\right] - \left[\begin{array}{l}\text{Mass of reactant}\\ \text{leaving volume}\\ \text{element}\end{array}\right] - \left[\begin{array}{l}\text{Mass of reactant}\\ \text{converted in the}\\ \text{volume element}\end{array}\right] \quad (1)$$

$$= \left[\begin{array}{l}\text{Accumulation of reactant}\\ \text{in the volume element}\end{array}\right] \quad \text{for a time element } \Delta t$$

and a volume element ΔV.

From this general mass balance the design equations for a back mix reactor and plug flow reactor can be derived.

The equation for the back mix reactor is:[14]

$$V_r = \frac{F_{AO} X_A}{-r_A} \quad (2)$$

where V_r = volume of reactor

$-r_A$ = rate for the particular reaction studied

F_{AO} = input of A moles/time

$$X_A = 1 - \left[\frac{\text{exit stream concentration } C_A}{\text{Input stream concentration } C_{AO}}\right].$$

Built into this equation are several assumptions that must be considered if the equation is to be valid. The volume

of the reactor is assumed to be constant as well as the density of the systems involved in the reaction. The above equation is also valid only when steady state in the reactor is reached. Figure 1a is a graphical representation of eq. 2.

In the plug flow reactor the composition of the fluid varies from point to point along the flow path so the material balance for the components must be made for a differential volume element ΔV. This balance can be made because there is no variation in properties or velocity in the radial direction. The derived equation[14] for a plug flow reactor is:

$$V_r = \int \frac{F_{AO} dX_A}{-r_A} \qquad (3)$$

where V_r = volume of reactor

$-r_A$ = reaction rate

F_{AO} = input of A moles/time

$$dX_A = \left[\frac{\text{exit stream conc. } C_A}{\text{input stream conc. } C_{AO}}\right].$$

There are also assumptions built into the derivation. They are:

1. The volume is not a function of time;
2. The concentrations are at steady state;
3. The reactor is of a plug flow type, i.e. the feed enters one end of a cylindrical tube and the product stream leaves the other;
4. Diffusion is negligible.

Figure 1b is a graphical representation of this equation. By superimposing Figures 1a and 1b it is shown in Figure

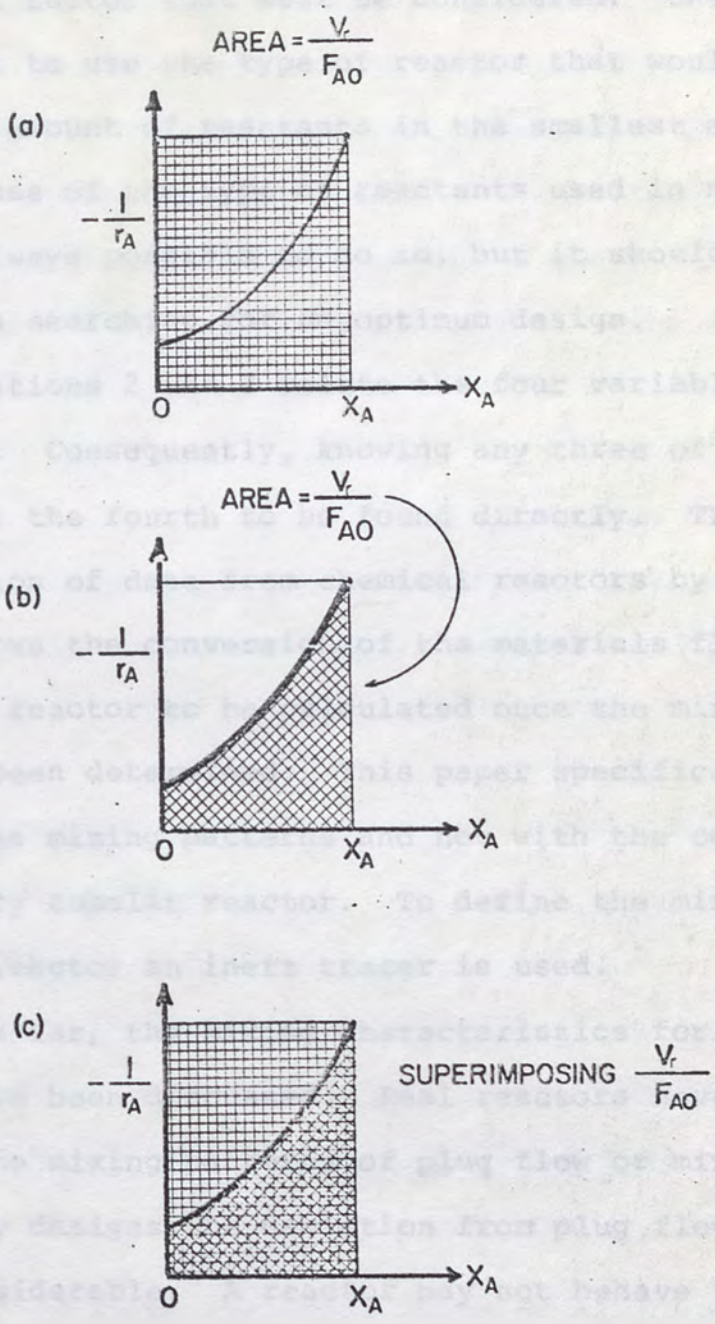

Figure 1: a) Graphical representation of the design equation for a back mix reactor.[14]

b) Graphical representation of the design equation for a plug flow reactor.[14]

c) Superimposing Figure 1a on 1b.[14]

lc that the plug flow volume V_r is always smaller than the back mix reactor volume.

When designing reactors for commercial uses, V_r is an important factor that must be considered. One would usually want to use the type of reactor that would process the largest amount of reactants in the smallest amount of area. Because of the type of reactants used in many cases, it is not always possible to do so, but it should never be ignored when searching for an optimum design.

Equations 2 and 3 relate the four variables X_A, $-r_A$, V_r, and F_{AO}. Consequently, knowing any three of the variables allows the fourth to be found directly. The ease of interpretation of data from chemical reactors by equations 2 and 3 allows the conversion of the materials flowing through the reactor to be calculated once the mixing patterns have been determined. This paper specifically deals only with the mixing patterns and not with the conversion of the rotary tubular reactor. To define the mixing patterns in a reactor an inert tracer is used.

Thus far, the mixing characteristics for two ideal reactors have been discussed. Real reactors never completely follow the mixing patterns of plug flow or mixed flow, and for many designs the deviation from plug flow and mixed flow is considerable. A reactor may not behave ideally because of: short circuiting, stagnant regions, bypassing, longitudinal mixing, or complete radial mixing. When studying a reactor to define its mixing properties, the residence

time distribution function must be considered. The residence time (θ) of a reactor is the time it takes a molecule to pass through the reactor. The residence time may be broken down into its age (the time elapsed since the molecule entered the reactor) and its residual lifetime (the remaining time it will spend in the reactor). The sum of the age and residual lifetime terms will be denoted θ. The residence time distribution function is the fraction $J(\theta)$ of the effluent stream that has a residual time less than (θ). Examples of the function are:

$$\text{at } \theta = 0 \qquad J = 0$$

$$\theta \to \infty \qquad J \to 1 \qquad \text{or } dJ(\theta) = 1$$

and can be shown graphically by Figure 2a. At constant density the mean residence time is defined as:[18]

$$\bar{\theta} = \frac{V/F_t}{p} = \frac{V}{Q}$$

where Q = flow rate (same in feed and effluent)

t = total flow rate

p = constant density

The shaded area in Figure 2a represents $J(\theta)$.

The RTD can also be described in terms of the slope of $J(\theta)$. This function is

$$J'(\theta) = \frac{dJ\theta}{d\theta} . \qquad (3a)$$

The curve produced by the $J'(\theta)$ function will have the shape usually associated with a normal distribution curve as shown in Figure 2b. From equation 3a the total area under the

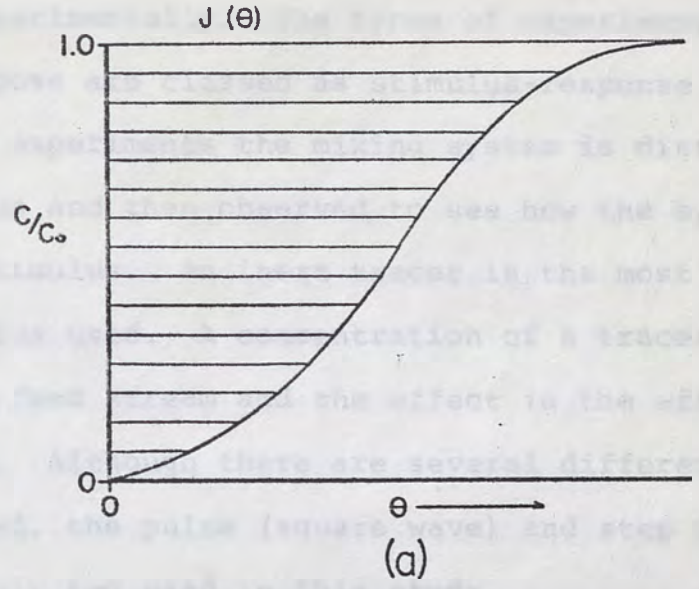

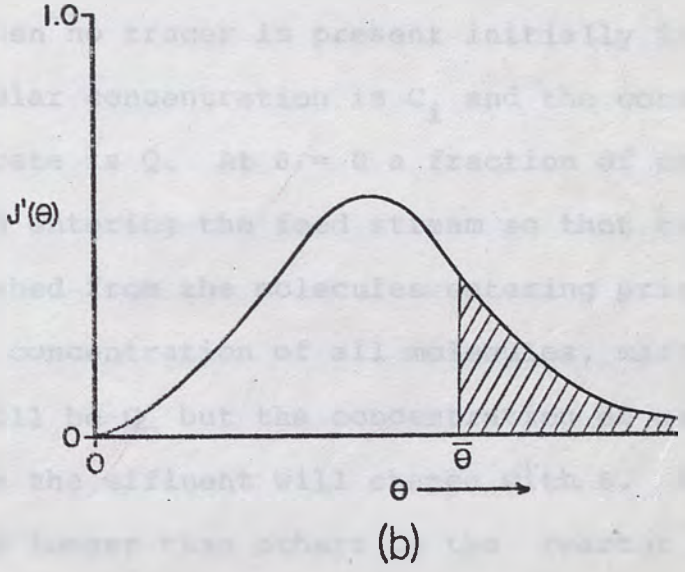

Figure 2: a) Typical effluent signal called the F curve or step input response. Slashed area is equal to $J(\theta)$.[18]

b) Typical effluent signal called the C curve or pulse input response. Slashed area is the fraction of the exit stream older than $\bar{\theta}$.

curve in Figure 2b is one, and the shaded area represents the fraction of the exit stream older than $\overline{\theta}$.

The extent of non-ideal flow may be characterized by the residence time distribution functions, which are found experimentally. The types of experiments used for this purpose are classed as stimulus-response techniques. In these experiments the mixing system is disturbed using a stimulus and then observed to see how the system responds to the stimulus. An inert tracer is the most common type of stimulus used. A concentration of a tracer is injected into the feed stream and the effect in the effluent is measured. Although there are several different perturbations used, the pulse (square wave) and step function will be the only two used in this study.

The step function will produce as a response an F curve. When no tracer is present initially in a stream, the molecular concentration is C_i and the constant volumetric flow rate is Q. At $\theta = 0$ a fraction of the molecules are marked entering the feed stream so that they may be distinguished from the molecules entering prior to $\theta = 0$. The total concentration of all molecules, marked and unmarked, will be C_o but the concentration of marked molecules C in the effluent will change with θ. Some molecules will spend longer than others in the reactor and can be shown by letting the response concentration ratio equal to C/C_o. The exact shape of the response curve depends on the mixing state of the system. At a time θ when the concentra-

tion of marked molecules in the effluent is C, flow rate of the marked molecules in the effluent is CQ. All marked molecules have entered the reactor in a time less than θ and by definition is the fraction of molecules that have this time (θ). Therefore:[18]

$$CQ = C_o Q J(\theta) \tag{4}$$

and

$$J(\theta) = \frac{C}{C_o \text{ step}} \tag{5}$$

Figure 3a shows an example of a step function input and a response curve.

The second type of stimulus, the pulse or square wave, has a response called the C curve. With no tracer present in the system an instantaneous pulse of tracer is imposed in the stream entering the reactor. The total number of marked molecules entering the reactor is:[18]

$$M = C_o Q \Delta t \text{ and } C = \begin{matrix} C_o \text{ for } 0<t<\Delta t_o \\ 0 \text{ for } t>\Delta t_o \\ 0 \text{ for } t<0 \end{matrix} \tag{6}$$

where Δt_o is the marking interval and C_o is the total concentration of marked molecules. Since C is the concentration of marked molecules at θ, the number of these molecules leaving the reactor in the time period θ to $(\theta + d\theta)$ will be $CQd\theta$. The fraction of the effluent stream consisting of these molecules is $dJ(\theta)$ or $J'(\theta)d\theta$. Therefore:[18]

$$CQd\theta = MJ'(\theta)d\theta \tag{7}$$

and

$$j'(\theta) = \frac{(C) \text{ pulse } Q}{M} \tag{8}$$

$J'(\theta)$ can be obtained from the response curve for a pulse input. Figure 3b shows an example of the pulse input and its response.

Reactors with known mixing characteristics such as the plug-flow reactor, a single ideal stirred tank reactor, and a tubular flow reactor with laminar flow, have RTD's that can be derived theoretically. To make these derivations one must refer back to the mass balance.

Because the conversion in a plug flow reactor is a function of the point along the length of the reactor, a plug flow reactor displays no axial mixing and a uniform velocity profile. The residence time of any particle in the reactor must be constant, $\theta = V/Q$. The curve response to a step function is shown graphically in Figure 4a. If $J(\theta) = (C/C_o)_{step}$ then for a plug flow reactor $J(\theta) = 0$ for $\theta < V/Q$ and $J(\theta) = 1$ for $\theta \geq V/Q$. The input and response curves for a pulse input correspond to narrow peaks at $\theta = 0$ and $\theta = V/Q$. Figure 4b is a graphic diagram of the response curve. The response curve of Figure 4b is proportional to $J'(\theta)$.

For the ideal stir tank reactor, $(C/C_o)_{step}$ may be calculated by applying the mass balance (Eq. 1) for a step function input. The third term of the mass balance is zero, since there is no reaction. At time θ, after the tracer concentration in the feed is increased to C_o, the other terms in the mass balance give:

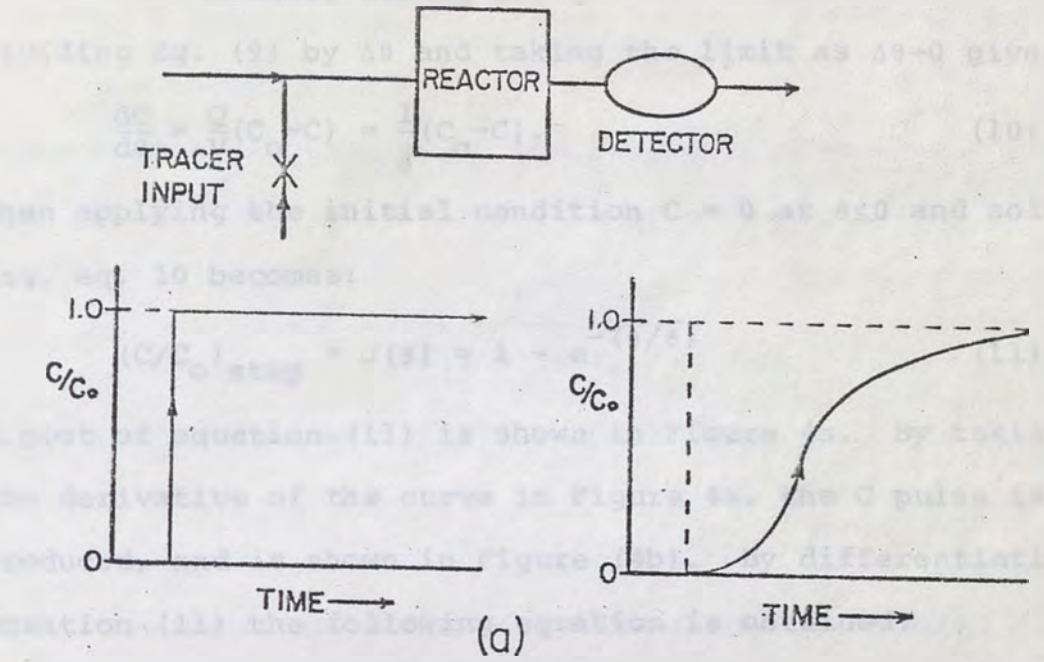

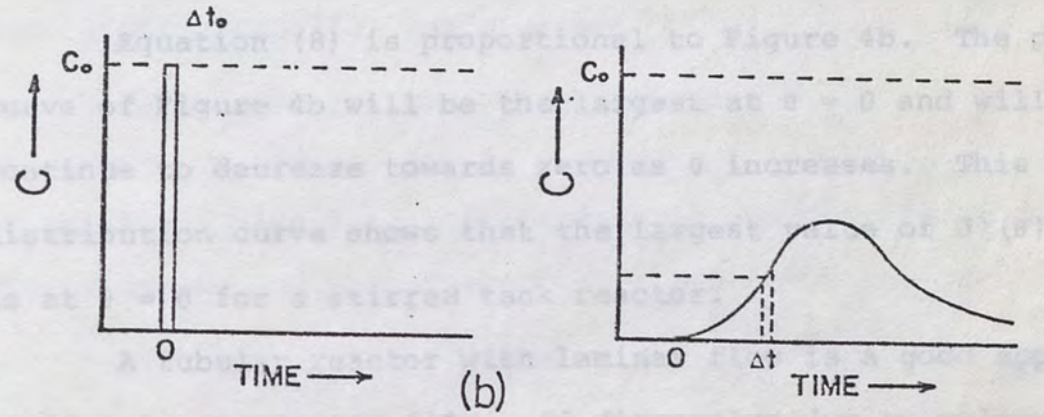

Figure 3: a) Reactor input stimuli and effluent response for a step input (F curve).[18]

b) Reactor input stimuli and effluent response for a pulse input (C curve).[18]

$$C_o Q\Delta\theta - CQ\Delta\theta = V\Delta C \qquad (9)$$

C = effluent concentration at θ

ΔC = change in concentration of tracer in the reactor during $\Delta\theta$.

Dividing Eq. (9) by $\Delta\theta$ and taking the limit as $\Delta\theta \to 0$ gives:

$$\frac{dC}{d\theta} = \frac{Q}{V}(C_o - C) = \frac{1}{\bar{\theta}}(C_o - C). \qquad (10)$$

When applying the initial condition C = 0 at $\theta \leq 0$ and solving, eq. 10 becomes:

$$(C/C_o)_{step} = J(\theta) = 1 - e^{-(\theta/\bar{\theta})} \qquad (11)$$

A plot of equation (11) is shown in Figure 4a. By taking the derivative of the curve in Figure 4a, the C pulse is produced, and is shown in Figure (4b). By differentiating equation (11) the following equation is obtained.

$$J'(\theta) = \frac{1}{\bar{\theta}} e^{-(\theta/\bar{\theta})} \qquad (12)$$

which is the equation for the curve in Figure (4b).

Equation (8) is proportional to Figure 4b. The pulse curve of Figure 4b will be the largest at $\theta = 0$ and will continue to decrease towards zero as θ increases. This distribution curve shows that the largest value of $J'(\theta)d\theta$ is at $\theta = 0$ for a stirred tank reactor.

A tubular reactor with laminar flow is a good approximation to segregated flow. If dispersion due to molecular diffusion is neglected, the approximation is exact. The RTD can be calculated from the known velocity profile of the segregated flow. The velocity in the axial direction for laminar flow is parabolic and is given as:

$$u(r) = \frac{2Q}{\pi r_o^2}[1 - (\frac{r}{r_o})^2] \qquad (13)$$

where r = radial position

r_o = tube radius

u = velocity.

Since u is a function of r, the residence time also varies with r. If the reactor length is L, θ at any r is

$$\theta = \frac{L}{u} = \frac{\pi r_o^2 L}{2Q[1 - (r/r_o)^2]} \qquad (14)$$

Since $L\pi r_o^2 = V$ equation (14) becomes

$$\theta = \frac{V/Q}{2[1 - (r/r_o)^2]} \qquad (15)$$

The fraction of the effluent stream of radius between r and (r + dr) will be:

$$dJ(r) = \frac{u(2\pi rdr)}{Q}. \qquad (16)$$

Substituting Eq. (13) for u gives:

$$dJ(r) = \frac{4}{r_o^2}[1 - (r/r_o)^2]rdr. \qquad (17)$$

To replace r with θ in this expression one must first differentiate Eq. 15 with respect to r and solve for rdr.

$$rdr = \frac{V}{4Q} \frac{r_o^2}{\theta^2} d\theta. \qquad (18)$$

Substituting $1 - (r/r_o)^2$ from Eq. (15) and rdr from Eq. (18), Eq. (17) yields:

$$dJ(\theta) = 1/2(\frac{V}{Q})^2 \frac{d\theta}{\theta^3} = 1/2\ \overline{\theta}^2 \frac{d\theta}{\theta^3}. \qquad (19)$$

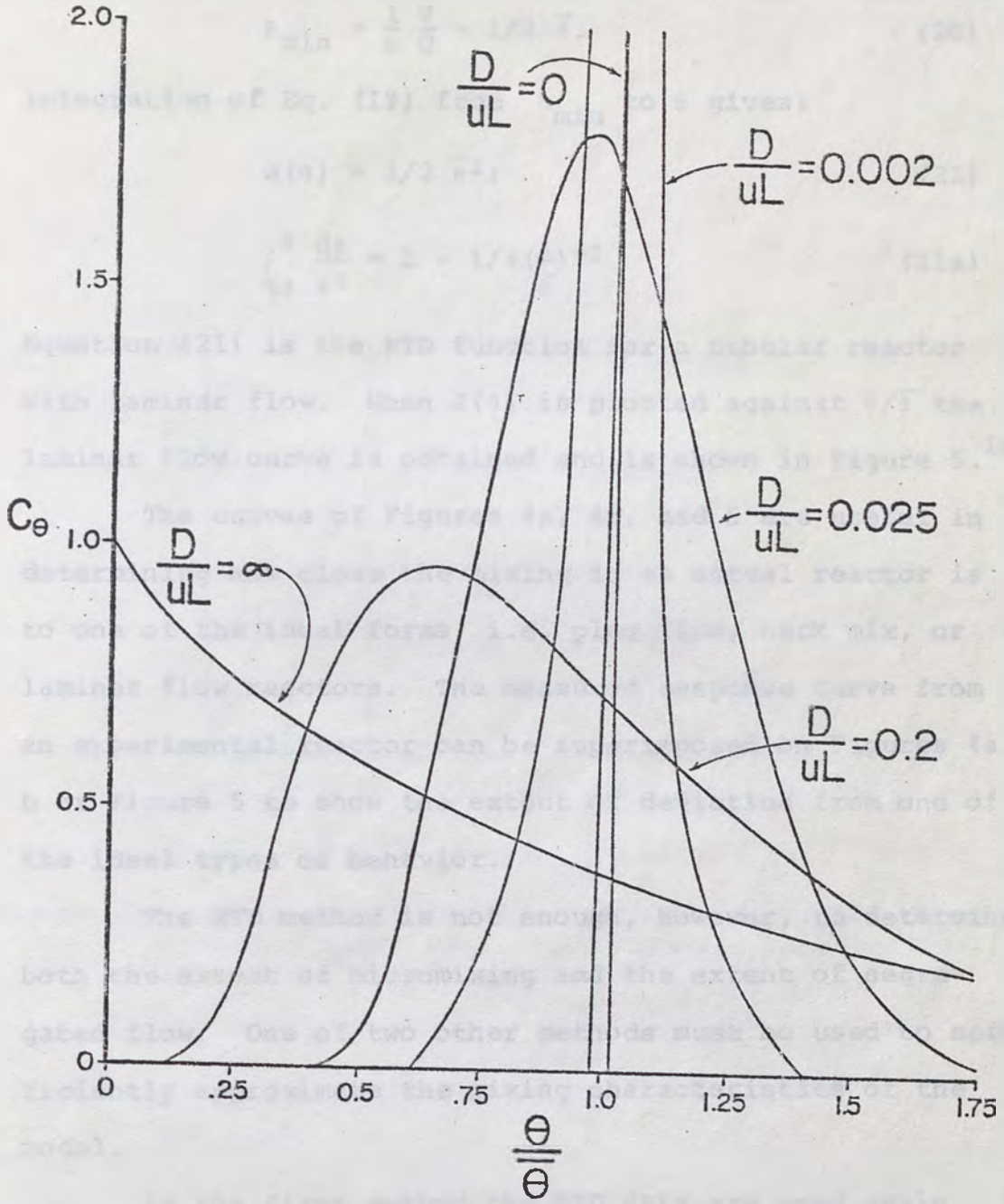

Figure 4: a) Properties of the F curve (step input) for various flows in terms of dimensionless time units.[14]

b) Properties of the C curve (pulse input) for various flows in terms of dimensionless time units.[14]

Integration of Eq. (19) gives $J(\theta)$. The minimum residence time is not zero but corresponds to the maximum velocity at the center of the tube.

$$\theta_{min} = \frac{1}{\theta} \frac{V}{Q} = 1/2\ \bar{\theta}. \tag{20}$$

Integration of Eq. (19) from θ_{min} to θ gives:

$$J(\theta) = 1/2\ \bar{\theta}^2; \tag{21}$$

$$\int_{\frac{1}{2}\theta}^{\theta} \frac{d\theta}{\theta^3} = 1 - 1/4\left(\frac{\theta}{\bar{\theta}}\right)^{-2} \tag{21a}$$

Equation (21) is the RTD function for a tubular reactor with laminar flow. When $J(\theta)$ is plotted against $\theta/\bar{\theta}$ the laminar flow curve is obtained and is shown in Figure 5.[18]

The curves of Figures 4a, 4b, and 5 are useful in determining how close the mixing in an actual reactor is to one of the ideal forms, i.e. plug flow, back mix, or laminar flow reactors. The measured response curve from an experimental reactor can be superimposed on Figures 4a, b or Figure 5 to show the extent of deviation from one of the ideal types of behavior.

The RTD method is not enough, however, to determine both the extent of micromixing and the extent of segregated flow. One of two other methods must be used to sufficiently approximate the mixing characteristics of the model.

In the first method the RTD data are used again, this time to calculate the axial diffusivity of the model, which is used to predict the reactor's mixing patterns.

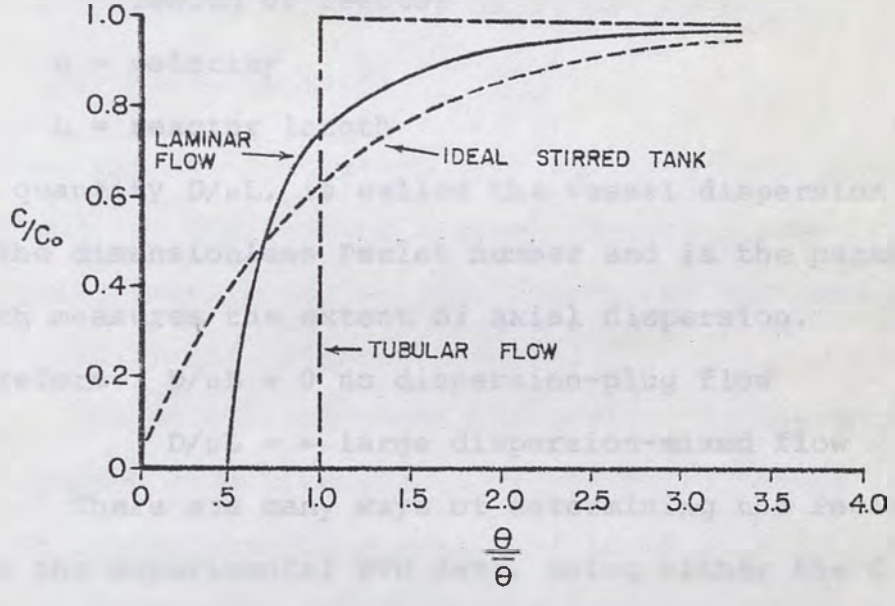

Figure 5: Comparison of responses from a step input for Tubular flow, Ideal Stir Tank and Laminar flow.[18]

The method of analyzing mixing patterns is known as the dispersion model. The theory proceding the determination of the vessel dispersion number originates from Fick's law. The proof will not be shown but the mathematical expression representing the dispersion model is:

$$\overline{\theta}\,\frac{\partial C}{\partial \theta} = \left(\frac{D}{\mu L}\right)\frac{\partial^2 C}{\partial Z^2} - \frac{\partial C}{\partial Z} \qquad (18)$$

where D = axial dispersion coefficient

$Z = \dfrac{\text{radial distance}}{\text{length of reactor}}$

u = velocity

L = reactor length

The quantity $D/\mu L$, is called the vessel dispersion number or the dimensionless Peclet number and is the parameter which measures the extent of axial dispersion.

Therefore: $D/\mu L \to 0$ no dispersion-plug flow

$D/\mu L \to \infty$ large dispersion-mixed flow

There are many ways of determining the Peclet number from the experimental RTD data, using either the C curve or the F curve. Only one method, using the data from the C curve, will be discussed.

If the pulse curve for the mixing of the reactor is quite unsymmetrical, any approximating methods are useless. A variance matching procedure is a common method for finding the Peclet number. The variance of a continuous distribution is measured at a finite number of equidistant locations on the curve.[14]

This gives:

$$\sigma^2 = \frac{\Sigma\theta_i^2 C_i}{\Sigma C_i} - \bar{\theta}^2 = \frac{\Sigma\theta_i^2 C_i}{\Sigma C_i} - \left[\frac{\Sigma\theta_i C_i}{\Sigma C_i}\right]^2 \qquad (23)$$

where σ^2 equals the variance of a tracer curve. By using the original tracer concentration and time data, ΣC_i, $\Sigma\theta_i C_i$ and $\Sigma\theta_i^2 C_i$ may be evaluated. By using the expression

$$\sigma_\theta^2 = \sigma^2/\bar{\theta}^2, \qquad (24)$$

σ_θ^2 may be calculated. For a closed vessel (a vessel with a change in flow patterns at boundaries):

$$\varepsilon_\theta^2 = 2\frac{D}{uL} - 2\left(\frac{D}{uL}\right)\left(1 - C^{\frac{-uL}{D}}\right) \qquad (25)$$

Solving the above equation by trial and error (D/uL) may be found for the reactor system. Figure 6 shows the curves in closed vessels for various extents of back mixing as predicted by the dispersion model.[14]

Two possible methods of modeling mixing characteristics have been discussed. In the third method the reactor is represented by a series of ideal stirred tanks of equal volume. The response data from the actual reactor are used to determine the number of tanks in series. For a given flow rate the total mean residence time is always the same. The residence time for each tank is therefore $\bar{\theta}_t/n$. Figure 7 describes the mixing pattern of a series of constant stir tank reactors. By comparing the response curves of the model to the curve of the actual reactor, the value of n can be found. The derived theoretical relationship between n and $(C/C_o)_{step}$ is:[18]

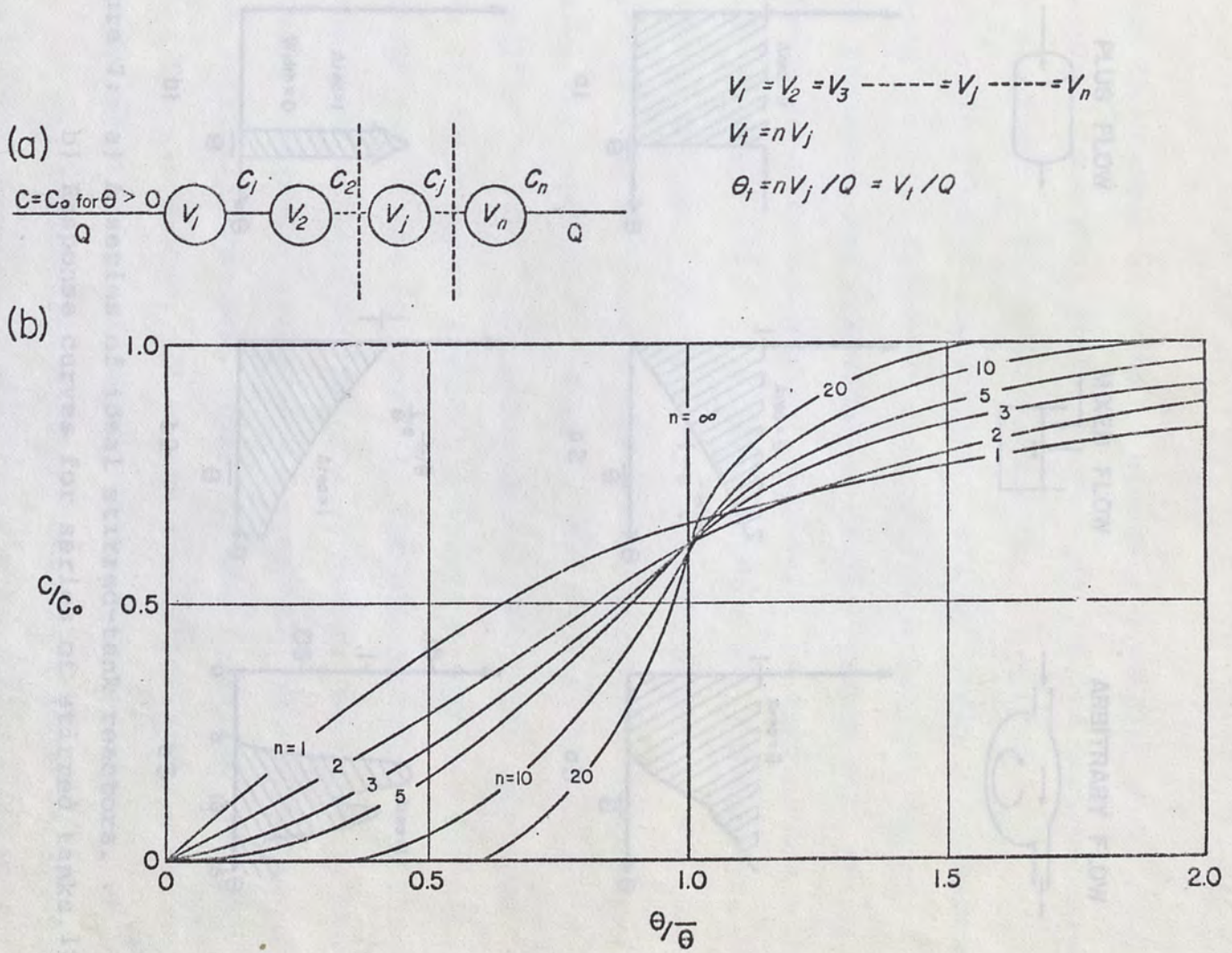

Figure 6: Pulse curves in closed vessels for various extents of back-mixing as predicted by the dispersion model.[14]

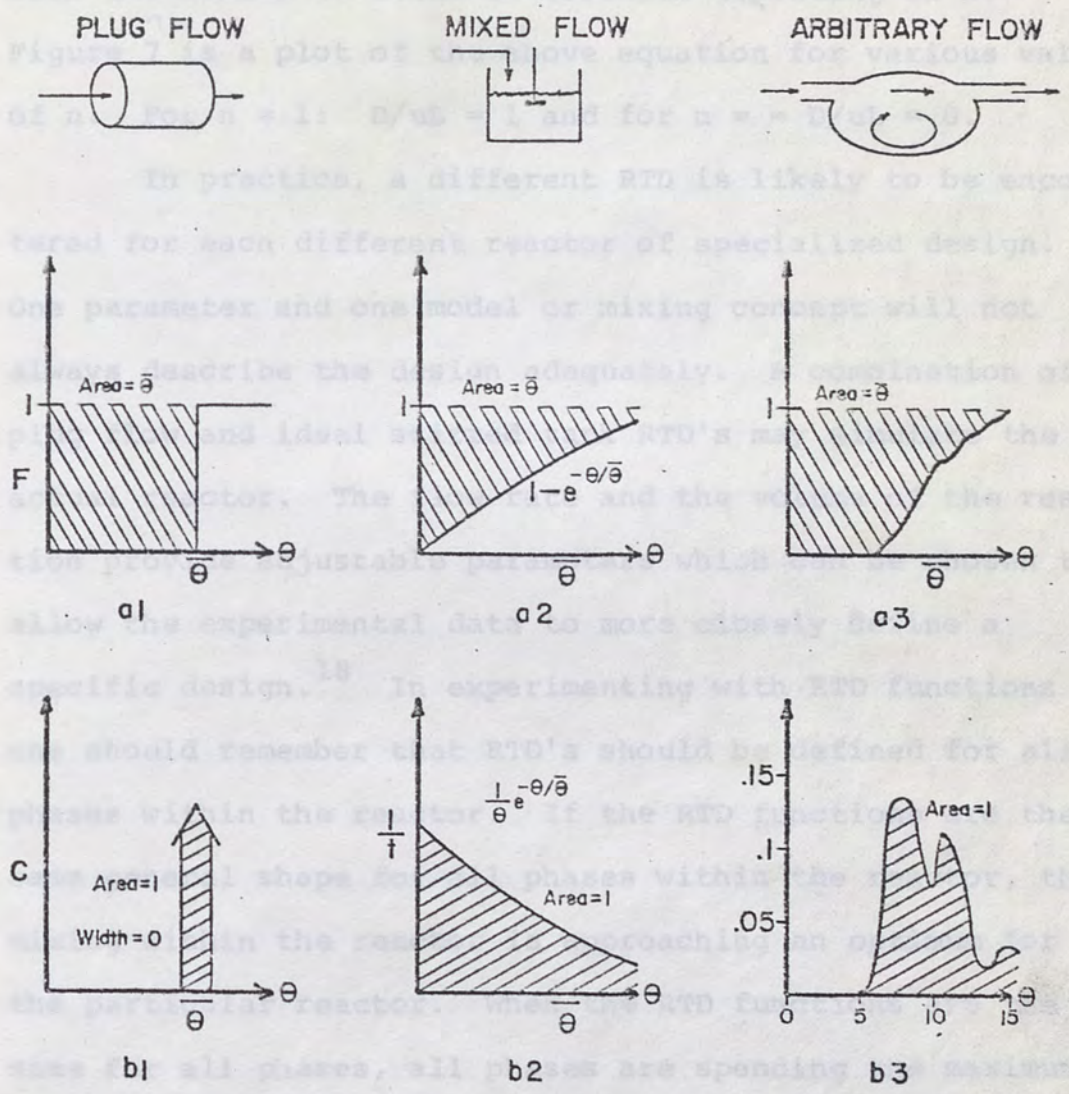

Figure 7: a) A series of ideal stirred-tank reactors.
b) Response curves for series of stirred tanks.[18]

$$(C_n/C_o)_{step} = J_n(\theta) =$$

$$1 - e^{-n\theta/\bar{\theta}_t}\left[1 + \frac{n\theta}{\bar{\theta}_t} + 1/2!\left(\frac{n\theta}{\bar{\theta}_t}\right)^2 + \cdots + \frac{1}{(n-1)!}\left(\frac{n\theta}{\bar{\theta}_t}\right)^{n-1}\right] \quad (26)$$

with the number of terms in brackets depending on n. Figure 7 is a plot of the above equation for various values of n. For n = 1: D/uL = 1 and for n = ∞ D/uL = 0.

In practice, a different RTD is likely to be encountered for each different reactor of specialized design. One parameter and one model or mixing concept will not always describe the design adequately. A combination of plug flow and ideal stirred tank RTD's may simulate the actual reactor. The flow rate and the volume of the reaction provide adjustable parameters which can be chosen to allow the experimental data to more closely define a specific design.[18] In experimenting with RTD functions one should remember that RTD's should be defined for all phases within the reactor. If the RTD functions are the same general shape for all phases within the reactor, the mixing within the reactor is approaching an optimum for the particular reactor. When the RTD functions are the same for all phases, all phases are spending the maximum amount of time simultaneously within the reactor.

The literature regarding mixing patterns is often conflicting because of unstated and unclear assumptions about what is happening at the vessel boundaries. Because of the conflicting theories, one should be careful when

using any RTD models, especially if the system is one in which fluid enters and leaves solely by plug flow, thus with a flat velocity profile.

EXPERIMENTAL DESIGN AND EQUIPMENT

A rotary tubular reactor was constructed from extrusive plexiglass. This material was chosen for its resistivity to acidic and alkaline solutions and for its non-abrasive properties. It was also readily obtainable and easy to handle. Plexiglass will bond to itself with the solvent, 1,2 dichloroethane. Because of this unique feature, the baffles were easily bonded to the inside of the tubular reactor.

The reactor was built from a 15.24 cm. outside diameter tube with a 0.635 cm. wall. Figure 8 is a schematic diagram of the reactor tube. The reactor was 120 cm. in length and was baffled with four 10 cm. by 2.8 cm. by 0.635 cm. baffles per cross section. Every cross section of baffles was rotated 45° from the previous section. The end of the tube was capped with a plate which contained a 2.54 cm. diameter hole for the liquids and solids to exit. These features are shown in Figure 9. The tube was baffled every 10 cm. with four baffles per cross sectional area with a total of forty-four baffles. The reactor intake housing consisted of a capped 10.16 cm. length piece of 10.16 cm. outside diameter plexiglass tubing. The end of the intake housing was capped with a 5.08 cm. diameter hole for a 5.08 cm. diameter tygon tubing to enter. The 5.08 cm. tygon tubing carried the liquids and solids from the feeder to the reactor. The exit housing

consisted of a piece of 15.24 cm. tubing with 10.16 cm. by 8.89 cm. port holes cut out for effluent discharge and to control splashing. This end was also capped. The discharge portholes were housed within a 20.32 cm. plexiglass tube with a 5.08 cm. perpendicular discharge tube for the liquids and solids. The discharge housing was held in place by a ring stand. This assembly was found to be the most practical with easy disassembly necessary because of frequent cleaning.

The stand for the reactor was also constructed from plexiglass and is schematically shown in Figure 10. The reactor itself was circumscribed by two plexiglass constraints that could be adjusted to any point along the reactor body by the use of set screws. The position of the reactor on the stand was maintained by the lubricated constraints. The reactor was cradled on four ball bearings mounted on the stand.

Mechanical equipment for rotating the reactor consisted of a Dayton split-phase model, 1/4 h.p., 1725 rpm motor. A 48 to 1 ratio Eberhardt model 1860 reducer, and various sized pulleys were used to gear the motor down to the specific rotations per minute needed. An "O" ring was used from the reducer to turn the reactor. The reactor and mechanical system were designed to handle loads up to approximately 100 pounds. Not more than 50 pounds of material was in the reactor at any one time. In the design an experimental safety factor of 2 was used.

The experimental constant stir tank was also built out of extrusive plexiglass. For this reactor a piece of 15.24 cm. outside diameter tubing 36.83 cm. long was used. The bottom was capped with plexiglass containing a 2.54 cm. hole and a 5.08 cm. in length piece of plexiglass tubing was bonded to the hole. This was used as a coupling for the attachment of 2.54 cm. tygon tubing for the effluent stream flow. The effluent was controlled by an adjustable C-clamp at the end of the tygon tubing. The effluent flow rate was adjusted to equal the influent flow rate. The tank contained four baffles extending the length of the tube to within 5.08 cm. from the bottom.

A 3.81 cm. diameter impeller was used. The size of the baffles and impeller, in relation to the tank diameter, were determined by consulting Brown[7] for the standard dimensionless modeling equations for the agitation in constant stir tanks. The rod from the impeller was turned by a Radiometer Copenhagen m-11 model laboratory motor. The motor was mounted on a ring stand to allow the height of the impeller to be varied. The top of the constant stir tank was not capped. The feed was dropped in through a 5.08 cm. piece of tygon tubing directly from the same feed system used for the rotary tubular reactor. The constant stir tank contained a 2.54 cm. hole at the maximum volume for overflow. The reaction volume of the constant stir tank was equivalent to the reaction volume of the rotary tubular reactor. Figure 11 is a schematic diagram of the

tank.

The experimental plug flow reactor was simulated by the rotary tubular reactor. The reactor was not rotated and consequently contained the same volume as the other reactor models.

The three reactors used for experimental purposes used the same feed system. The system consisted of a Denver revolving pulp feeder model ZW run by a General Electric 1/4 h.p. 1725 rpm motor. The input of solids was controlled by the rotation rate of a plate underneath the conical hopper and by the angle of the vertical plate scraper. The liquids were stored in five gallon Nalgene bottles and pumped into the system through a Cole Parmer Masterflex model 7016 peristaltic pump. After solids were dropped from the revolving plate they were washed down into the inlet tubing by the liquids. Once the solid feed rate was constant, the solid liquid ratio could be altered by changing the liquid flow rate.

Three other pieces of equipment were used in collecting experimental data. A Bausch Lomb Spectronic 70 spectrophotometer was used for all spectrophotometric work. A Perkin Elmer atomic absorption machine, model 303, was used for the analysis of copper and molybdenum. The measurement of concentrations of the naturally occurring radioactive materials was done with a RIDL model 34-12B radioactive counter. For some of the calculations, the University of Nevada Computing System was used. Programs

were run in Fortran IV language. No other equipment was used in the course of experimentation.

EXPERIMENTAL REAGENTS AND ORES

For the duration of experiments, ore from the Henderson, Colorado mine of the Climax Molybdenum Company was used. It consisted mostly of monzonite and quartz. A chemical analysis on a mass spectrometer by the United States Bureau of Mines gave the following results:

Mo - 0.25 percent
Fe - 1.50 percent

Only traces of other elements were present, and the density was found to be 2.71.

This ore was "salted" with a molybdenum concentrate from Kennecott Copper Corporation, until a level of 0.5 percent molybdenum was reached. This mix was then ground in a laboratory size steel ball mill. All ore used for experimentation was rolled in large containers for three hours.

For the chalcopyrite-sulfuric acid leach, the monzonite inert ore was "salted" with a 30 percent copper Kennecott Copper concentrate which contained a mineral structure of chalcopyrite. The final analysis of the experimental ore contained 4.0 percent total copper. This experimental mix was handled in the same manner as the other mix and a sieve-test produced size fractions given in Tables I & II. By comparing both tables, it is shown that all ore used for experimentation had approximately the same sieve analysis.

The tracer used for all liquid residence time distribution tests was nickel chloride (NiCl). A saturated solution of NiCl was made from solid 99.8 percent pure NiCl. Tap water was used at all times as the liquid phase unless otherwise specified.

Two solid tracers were used. The first was a naturally occurring radioactive thorite ($ThSiO_4$). The thorite used had a half life ($t_{\frac{1}{2}}$) of 1.39×10^{10} years, and its spectra was very complex because of daughter products. The thorite was 100 percent plus 100 mesh and is classified as the non-slime tracer. The second tracer used was naturally occurring radioactive pitchblend (U_3O_8). The half life of the pitchblend was 4.5×10^9 years and also had a complex spectra because of daughter products. Pitchblend was 100 percent minus 325 mesh with slimy characteristics. It is denoted as the slimy tracer. The thorite possessed 39.9 percent of the gamma counts of the pitchblend, so smaller amounts of pitchblend were used in all experimental tests. This procedure was done so that approximately the same number of counts were used in each experiment.

All radioactive material was supplied by the United States Bureau of Mines.

The reactants used for experimentation included a 14 percent sodium hypochlorite (NaOCl) reagent in the molybdenum sodium hypochlorite leach. The sodium hypochlorite was diluted to 3 percent by volume which left an excess

amount of reagent after the reaction was completed. Concentrated sulfuric acid was used for the chalcopyrite leach. This reagent was diluted by volume with water to 1 N which also gave an excess of reagent.

EXPERIMENTAL PROCEDURE

After the reactor was constructed and in working order, its volume was measured. This feat was accomplished by filling the reactor with water and measuring the volume of water contained. The residence time of the experiment ($\bar{\theta}=V/Q$) was calculated and was a function of the flow rate as the volume of the reactor remained constant. The behavior of the flow of solids and liquids was checked against the mass balance equation, (in = out; at steady state).

Ore and water were fed into the reactor until a steady stream of liquids and solids were discharged. At this point all material entering the reactor appeared to be discharging and steady state was predicted. To confirm this prediction all material coming out of the reactor for one hour was collected and weighed. The sample was then placed in a drying oven and all water was evaporated off leaving only the solids. The solids were weighed resulting in both solids and liquids comparing equally with the initial amounts of feed.

The first residence time distribution function curves obtained were for liquids. A tracer consisting of a saturated solution of NiCl was used. For the pulse curves the reactor was allowed to reach steady state conditions with a feed of water and ore. A pulse consisting of 250 ml. of saturated NiCl solution was measured for an absorbance reading on the spectrophotometer at 690 nm.

The above pulse was then injected into the fluid stream. The instant at which the fluid was injected into the stream was established as time (t) equal zero. Samples were taken every five minutes from t equal zero and filtered using No. 2 Watman Filter Paper. The absorbance of the filtrate was read at 690 nm. on a spectrophotometer against a blank that was obtained from the reactor before the pulse was injected. The absorbance was normalized by expressing it as a fraction of the initial absorbance of the pulse before it was injected. The experimental variable was the rotation speed and tests were conducted at 24, 14, 7 and 4.5 rotations per minute.

The liquid step function tests were conducted in a similar manner. The reactor was allowed to reach steady state with a feed of water and ore. At that time the liquids were switched from water to a solution of NiCl. From that time (t=0) samples were taken every five minutes, filtered, and read on a spectrophotometer at 690 nm. When the point was reached where the absorbance did not change, the experiment was terminated. The absorbance readings were normalized by expressing them as a fraction of the constant last absorbance taken. All step input tests were run at 14 rotations per minute.

A soluble mineral test was conducted using sodium hypochlorite and molybdenum sulfide "salted" ore. The reactor speed was constant at 14 rpm. A tracer pulse of 30 g. of 30 percent MoS_2 was injected into the feed stream.

Samples were taken every 5 minutes, filtered, and analyzed for molybdenum using a Perkin-Elmer 303 atomic absorption spectrophotometer.

A standard procedure as detailed by Perkin-Elmer was followed.[17] Concentration in the effluent stream was normalized by expressing it as a fraction of the total concentration injected into the feed stream.

The residence time distribution curve produced by the soluble mineral test was compared with the 14 rpm liquid phase residence time distribution curve. The comparison was made to show the similarity between the flow patterns of water with an inert ore and a leach solution with leached ore.

Residence time curves for solids were experimentally produced much in the same manner as the liquid residence time step and pulse curves. After the reactor reached steady state with a water-ore feed, a pulse of 15 g. of non-slimy thorite was injected into the feed stream. A two-minute sample was taken every 15 minutes starting at t=0 for 390 minutes. Samples were dried in a drying oven at 180°F until complete dryness. Samples were then read on a radioactive counter at the United States Bureau of Mines radioactive laboratory. The effluent counts were normalized by expressing them as a fraction of the total number of counts in the exit stream from the beginning of sampling to the end. The pulse tracer test for the slimy material was conducted in the same manner using 5 g. of radioactive

pitchblend as the tracer. In both the slimy and non-slimy pulse tests the rotation speeds were varied. The tests were performed at 22, 14, 7 and 4.5 rpm.

The step function tests for the solids utilized a slightly more complicated procedure. The initial step to this experiment was to prepare the feed for the run containing the tracer. Thirty grams of thorite in the non-slime case was rolled with 3000 grams of inert feed for complete mixing. The reactor was allowed to reach steady state with a water-ore feed. At this point the system was shut down completely for approximately 15-20 minutes. The feeder was cleaned and blown free of dust with compressed air. The new feed containing the radioactive tracer was transferred to the feeder and the complete system was re-started. Samples were taken every 15 minutes for 100 minutes. Samples were dried as previously stated in the procedure and counted using the United States Bureau of Mines radioactivity counter. Effluent concentrations were normalized by expressing them as a fraction of the steady state concentration attained by the tracer.

The chalcopyrite-sulfuric acid leaches were conducted by pumping a 1 N sulfuric acid solution and feeding a 4 percent total copper mix into the reactor. The solid-liquid ratio was one of two variables considered. Ratios tested for performance were 1:4, 1:13, and 1:8 solids to liquids. Besides varying the solid-liquid ratios, the rotation speed was varied. Rotation speeds used for

experimentation ranged from 4.5 rpm to 24 rpm. The same solid-liquid tests were run in the constant stir tank and the simulated plug flow reactor. Once a reactor had reached a steady state in each run, samples were taken at 5 minute intervals. Samples were filtered through Wattman #2 filter paper and analyzed for copper on a Perkin Elmer 303 atomic absorption spectrophotometer.[17] Concentrations were normalized by expressing them as a fraction of the total copper concentration in the ore, diluted to the proper solid-liquid ratio. A total of 22 runs were performed in this experimentation.

RESULTS

Table III contains data from the liquid step function tests. Two runs were made under the same conditions and they were averaged together for the final set of C/C_o data. Standard conditions were a 1:10 solid-liquid ratio and 14 rpm. The results are plotted on Figure 12. The liquid F curve begins at $\theta/\bar{\theta}=0$ but between $\theta/\bar{\theta}=0.3$ and $\theta/\bar{\theta}=0.8$ the curve has the general convex properties of a laminar flow curve. The F curve approaches $C/C_o=1$ at $\theta/\bar{\theta}=1.45$.

Table IV contains data from the solid step function tests. The conditions under which these runs were made were 1:10 solid-liquid ratio and 14 rpm. The residence time of the actual experiment was different in each case, but was expressed as a normalized function $\theta/\bar{\theta}$. Several runs were made and averaged because of the error involved with the feeder. Figure 13 is a plot of the solid step function tests. The curve starts $\theta/\bar{\theta}=0$ and approaches $C/C_o=1$ at $1.50\theta/\bar{\theta}$. It does not have the shape of either the ideal plug flow reactor or the back mix reactor F curves.

Figure 14 compares the liquid step function curve to the solids step function curve. Both curves start at the origin. The important point of this graph is that the curves both become asymptotic at approximately the same $\theta/\bar{\theta}$. There is deviation in the curves between $\theta/\bar{\theta}=0.3$ to $\theta/\bar{\theta}=0.8$.

Tables V and VI contain the data from the liquid pulse tests. Several runs were made at 14 rpm (Table V) in order to determine the deviation involved in pulse curve tests. Since the error was negligible, the runs at 24, 14, 7.5 rpm were not repeated. Figure 15 is a graph comparing the pulse curves of the various rotation speeds. The solid-liquid ratio was 1:10 in all cases. All curves start at $\theta/\bar{\theta}=0$. Figure 15 illustrates that the peak shift is a function of the rotation speed. There is a deviation in the height of the curves of approximately 30 percent. An average C/C_o value of approximately 0.98 was noted for further comparison.

Table VII contains the data for the soluble mineral pulse response curve. Two runs were made and averaging the data produced the points for the curve in Figure 16. Note that the maximum point on the curve occurs at $\theta/\bar{\theta}=0.30$ and at a value of C/C_o of 0.63. Soluble mineral tests were run at 1:10 solid-liquid ratio and at 14 rpm.

Comparison of the 14 rpm curve of Figure 15 with the curve of Figure 16 produces Figure 17. The maximum points on the curves of both plots are at approximately the same $\theta/\bar{\theta}$. Both curves demonstrate the same general shape.

Figure 18 was generated by comparing the 14 rpm curve of Figure 15 with a new curve generated by considering the initial turbulence from the tracer input within the reactor. The initial turbulence, when tracers were

injected, appeared to be only in the first 20 cm. of the 120 cm. reactor. The volume of the reactor used for calculating turbulence was determined by subtracting the approximate volume containing the colored tracer at t equal zero from the total volume. In the turbulence calculations, a new volume of 5/6 the original volume was used. A new mean residence time V/Q was calculated. Times were normalized using the new residence time and plotted against the original C/C_o values of the 14 rpm curve in Figure 15. The curve is slightly shifted to the left, with the maximum of the curve at $\theta/\bar{\theta}=0.05$ to the left of the original. Table VIII contains the data used to plot Figure 18.

Table IX contains data for the non-slime solid pulse input tests. Thorite, 100 percent + 100 mesh (non-slime), was the tracer used and the rotation speed was varied. The solid-liquid ratio remained 1:10 throughout the experiment. Figure 19 is a plot of the three rotation speeds tested. All curves are similar in shape with the average peak height at 0.074 C/C_o. This is very low in relation to Figure 10 and the other liquid RTD plots. The non-slime experimental peak is shifted to the right of the liquid pulse curves with the average at approximately $\theta/\bar{\theta}=2$.

Table X contains the data for the other set of solid pulse input tests. Pitchblend, 100 percent - 325 mesh (slime), was used as the tracer again. The rotation speed in this case was also varied and the solid liquid ratio remained at 1:10. Figure 20 is a plot of the data

in Table X. The figure shows that all of the curve maxima fall at the same value of $\theta/\overline{\theta}$, which is approximately 0.6. All curves have the same general shape with the average height being $C/C_o = 0.24$. The only curve that deviates from the other three is the 4.5 rpm curve.

Figure 21 is a plot of the slime RTD vs. the non-slime RTD. The slime RTD has a maximum peak three times the height of the non-slime maximum. The maximum of the slime curve also falls approximately $\theta/\overline{\theta} = 1.3$ to the left of the non-slime curves.

Figure 22 is a comparison of the solid slime and non-slime RTD's with the liquid RTD superimposed. All curves were generated at 14 rpm and at a liquid solid ratio of 1:10. The maximum points on all three curves are at different $\theta/\overline{\theta}$ values. The liquid curve maximum is the closest to the slimes maximum in terms of $\theta/\overline{\theta}$. They are $\theta/\overline{\theta} = 0.43$ units apart. The general shapes of the curves differ from each other.

Table XI contains the data that were used in calculating the Peclet number for the slime and non-slime solid pulse curves. The method used was the variance method discussed in the theory section. The Peclet numbers are calculated directly from experimental data in Appendix I. The Peclet values for the experimental curves along with the experimental solid pulse curves are plotted on Figure 23. Figure 23 is essentially the same plot as Figure 6 but in Figure 23 a graphic comparison is made between the

experimental values and the theoretical values. Note should be taken of the maximum on each curve in comparison to $\theta/\overline{\theta}$.

Appendix II contains the computer program for determining the curve for an arbitrary value of n constant stir tanks in series. The program was run for n = 1 to 20 and at various values of $\theta/\overline{\theta}$. Four of the curves generated from the data in Appendix II are plotted in Figure 24. Figure 7 is essentially the same plot but because it was not graphically accurate the curves had to be regenerated from the equation. All curves asymptotically approach 1 at different points and each curve does not begin at the same point on the x axis. Since all the experimental solid step function data began at zero, the theoretical curves were shifted to zero so that a comparison could be made of the general shapes as is shown in Figure 25. This procedure will be justified in the discussion. The experimental curve is superimposed on the theoretical curves for n = 20, n = 10, and n = 9. The experimental curve closely resembles those of 9 or 10 constant stir tank in series models. At some points the experimental curve falls directly between the theoretical curves of interest. There is a slight deviation between the curves from $\theta/\overline{\theta}$ = 0.5 to $\theta/\overline{\theta}$ = 0.9.

Table XII contains the data from the chalcopyrite-sulfuric acid leach tests. It is classified in relation to the solid-liquid ratio with leach ability measured as percent copper extracted. Figure 26 is a plot of this data. The maximum point of the 1:4 solid-liquid ratio

curve falls at 22 rpm, the maximum of the 1:13 curve at 14 rpm and the maximum of the 1:8 ratio at 18 rpm. The trend of increasing optimum rotation speeds with a decrease in the solid-liquid ratio is graphically shown. Figure 27 is a plot also using the data of Table XII. The constant stir tank and plug flow extraction data are compared to rotary tubular reactor extraction data. This graph definitely shows that at any solid-liquid ratio more copper was extracted in the rotary tubular reactor. The constant stir tank produces a much lower extraction but it still does slightly better than the plug flow reactor.

DISCUSSION

Three distinct methods (RTD method, dispersion method, and n-constant stir tank method) for estimating deviations from ideal reactor performance have been applied to the experimental data from the rotary tubular reactor.[18] Each one of these methods separately has not produced enough information to define the mixing parameters of the reactor. By combining all three methods, however, the extent of both micromixing and segregated flow has been predicted.

By comparing the step function response curves for liquids and solids in the rotary tubular reactor (Figure 14) one can see that the curves approach one another at the same $\theta/\bar{\theta}$. This result indicates that both liquids and solids entering the reactor at time t = 0 will exit simultaneously. The phenomena shows that a maximum amount of internal mixing was taking place. Theoretically maximum mixing will take place in the shortest amount of time if all species involved are in contact with each other at all times. However, the liquid step curve (Figure 12) indicates by its shape signs of approaching plug flow behavior in the range of $\theta/\bar{\theta}$ = 0.6 to $\theta/\bar{\theta}$ = 1.1. The liquid step function curve crosses the line $\theta/\bar{\theta}$ = 1 at C/C_o = 0.95. At the mean residence time $\bar{\theta}$, 95 percent of the effluent stream has a residence time less than the mean value. The value of the step function of the ideal stirred tank at

this same point is 0.631 or 63.1 percent and the value of the laminar flow step function curve is 0.78 or 78 percent. By comparing the three numbers, one can see that the 95 percent is much higher than the laminar flow or back mix reactor percentages. It is the closest, to the value given for ideal tubular flow, 100 percent. Since the experimental curve does not start at $\theta/\overline{\theta} = 0.5$, a complete laminar flow pattern was not considered. An ideal plug flow mixing pattern was not considered because the experimental curve did not start at $\theta/\overline{\theta} = 1$ and increase to $C/C_o = 1$ at $\theta/\overline{\theta} = 1$. The curve for the baffled rotary tubular reactor illustrates, however, that a combination of tubular flow and back mix patterns are taking place within the reactor. They are characterized by the presence of both axial and radial mixing states.

The solids step function curve (Figure 13) shows that for the solids, the reactor performance is again related to those of both ideal back mix and the plug flow reactors. Laminar flow of the solids was ruled out because of curve shape. Pulse curves for the reactor had to be considered before any definite mixing patterns could be defined.

When considering the pulse response curves for the liquids, the mixing conditions were defined directly from the position of a particular curve in relation to ideal curves. For optimum mixing in the axial direction the curve should approach the ideal back mix reactor curve as

shown in Figure 4b2. For optimum mixing in the radial direction experimental curves must approach the ideal plug flow curve of Figure 4b1. Mixing in both the radial and axial directions will be at an optimum when the experimental curve lies between the two ideal curves. By looking at Figure 15 it is seen that the maxima on all the experimental curves fall between $\theta/\overline{\theta} = 0$ and $\theta/\overline{\theta} = 1$. Thus all experimental curves are approaching the conditions of good mixing in both the axial and radial directions. The 4.5 rpm and 7 rpm curves seem to fall closest to the middle (about 0.5) and in the author's opinion these rotation speeds give rise to the best mixing because there is an equal amount of radial and axial mixing taking place within the reactor. In the author's opinion the variance in height of the peaks is not a function of mixing but is a function of the experimental error. The mixing is a function of the rotation speed as long as the density of the feed remains constant. If the rotational speed of the reactor is too fast for the density of the feed, the slimy mixture within the reactor will become centrifuged to the internal surface of the reactor. If the centrifugal force applied to these particles is too large, the tumbling action of the reactor will not prevent a greater equal and opposite force to cause the particles to leave the walls of the reactor. For the specific ore (density 2.7) and fluid (density 1) used in this experimentation, the optimum rotation speed seemed to be 7 rpm.

The liquid residence time distribution curves of the turbulence tests were then compared to the liquid pulse curves for an evaluation of error involved in the horizontal shift of the curves. Figure 18 shows the shift when an initial turbulence involving 1/6 of the reactor is considered. The turbulence in this test only shifted the curve $\theta/\bar{\theta} = 0.03$ in the horizontal direction. Therefore, the liquid pulse curves themselves are quite accurate and possess little experimental error. Any experimental turbulence caused by an unsteady flow rate or vibration from the mechanical system should not produce any more turbulence than the test did when it involved 1/6 of the reactor.

The second set of tests compared the flow patterns of the solutions before and after they contained soluble mineral. Figure 17 shows that the curves before and after addition of soluble mineral are very similar with the maximum of both curves in an exact vertical line. Therefore, the liquids in the reactor may be treated as having the same flow pattern before and after the minerals have been leached within the reactor.

The results from both the liquid and solid pulse tests determine the mixing patterns. A literature search reveals[2,12] that previous research has been conducted on only one phase continuous systems. The liquid has been the only phase considered experimentally. With the rotary tubular reactor, two continuous phases must be considered. If the liquid RTD produced simulates the solid RTD

produced, then the system is exhibiting perfect mixing.

By comparing the solid RTD pulse curves, (Figure 19), one can see where the horizontal shifting is again a function of the rotation speed of the curve maximum. In this case the 22 rpm curve is shifted more to the left. But, take note of where the average $\theta/\bar{\theta}$ lies for the maxima. It is in the vicinity of $\theta/\bar{\theta} = 2$. In comparison with the liquid curves, the solid pulse curves are shifted 1.38 $\theta/\bar{\theta}$ units to the right. The overall height of the curve is one order of magnitude less than the height of the liquid pulse curve. The curves fit the general shape of the set of liquid pulse curves but graphically are not positioned in the same place on the axis. Comparing the experimental solid pulse curves to the ideal mixing curves of Figure 4 it appears that the mixing patterns of the solid RTD are closer to the plug flow type than to the back mix type.

Thus far, two conflicting theories have developed. The step function response for the liquids and solids shows good mixing with the mixing pattern somewhere between plug flow and stirred tank behavior. The liquids pulse data also show good mixing with its mixing patterns indicating both axial and radial mixing. The solid pulse data show fair mixing with plug flow behavior being approached. Because of conflicting theories another type of modeling must be used to help predict the mixing.

The dispersion model was used to help predict the mixing states. A Peclet number was calculated for the non-slime solid pulse curve. A plot of this experimental curve is one of two curves on Figure 23 and is labeled as non-slime. By remembering that at $D/uL = 0$ when plug flow behavior is approached and $D/uL = \infty$ when mixed flow is approached, one can compare the experimental curve to ideal curves. The Peclet number for the experimental curve is 2.5. Thus, the flow pattern in the reactor does not display plug flow behavior. According to Levenspiel[14] a Peclet number of equal to or greater than 0.2 "displays a large amount of dispersion". The axial dispersion of the liquids is not considered because the liquid solid ratio was such that the solids were dispersing in a large amount of liquid. The dispersion model therefore shows that the solids disperse very well in the rotary tubular reactor.

Because there is still some question as to the validity of the above discussion, a third method of determining the mixing states was attempted. This is the series-of-stirred-tanks model. By consulting Figure 25 it is seen that the rotary tubular reactor solid step function curve has the same general shape as the theoretical curve for nine or ten constant stir tanks in series. In order to compare the shape of the curves the theoretical curves were shifted to $\theta/\bar{\theta} = 0$ and the experimental curve was superimposed.

In the author's opinion, this shift could be made because:

1. Only the shapes and overall width of the theoretical curves were compared to the experimental curves.

2. The placement of the experimental curves in relation to the x axis is a function of a large amount of error. Experimentally, it was impossible to begin measuring the effluent stream at the instant the tracer was injected. In many cases a sample was not taken for five to ten minutes after the tracer was injected. When curves were plotted they were automatically extrapolated to zero. In most cases considered, the curve was only shifted 0.25 units of $\theta/\overline{\theta}$. If the reactor had a 36 minute residence time, this curve shift would only amount to nine minutes.

The solid phase was the only phase considered in this modeling because of the large solid-liquid ratio. As stated before, the solids disperse in a large amount of liquid. If the solid-liquid ratio were in the vicinity of 1:2, it would be necessary to consider the liquid step function models. The solid-liquid ratio used for this experimentation was 1:10.

It is known that $n = 1$ for $D/uL = \infty$ and $n = \infty$ for $D/uL = 0$. These relationships are shown in Figure 7. The Peclet number agrees with the experimental n-constant stir tank modeling numbers quite well. In summary of the previous discussion, the rotary tubular reactor possesses mixing characteristics which have many of the properties

of both the plug flow and the back mix reactors. The mixing characteristics can be modeled after nine or ten constant stir tanks in series. If the conditions were found such that the liquid and solid pulse functions were approximately the same, the best mixing states for the reactor would occur.

The determination of the general residence time distribution functions of the rotary tubular reactor was the first step in determining the effect of slimy ores on the reactor. To study the effect of slimes, a solid pulse test was run with the pulse of tracer being a slimy pitchblend. The graphical results of these tests shown in Figures 20 and 21 indicate that the reactor handles the slimes in a different manner from the non-slimes. The response curve for the slimes is approximately $C/C_o = 0.14$ higher and shifted $\theta/\overline{\theta} = 1.3$ to the left. There is better axial mixing with the slimes and the peak shift is not a function of the rotational speed. The particles in the slimes are so small that it would most likely take a centrifugal force greater than could be produced by a reactor under the given conditions to centrifuge the particles to the inner walls. The dispersion model was also used to define the mixing pattern of the slimes. The Peclet number was calculated by the variance method to be 3.8. When the curve was plotted on the graph of Figure 23 it was shown that the curve peak is shifted further to the left of the non-slime peak. The Peclet number is also larger

and therefore more dispersion is taking place with the slimes in comparison to the non-slimes.

Figure 28 is a photograph of the reactor containing the slimes. The slimes do stick to the sides of the reactor and on to the baffles, but as the reactor turns, the wave motion produced by the baffles splash up and disperse any particles on the baffles. The wave motion produced in the reactor (Figure 29) is a function of the number of cross sectional sets of baffles contained within the reactor. To the author's speculation the modeling of the reactor is a function of the number of baffles in the reactor. Each baffle produces a small flow pattern completely of its own that resembles the flow pattern of a baffled constant stir tank. With the reactor rotating, there is little chance that any of the slimy particles will remain unreacted. Also combined into the flow patterns are the plug flow characteristics of a long tubular reactor. The combination of all these distinct characteristics have produced a hydrometallurgical device which in the author's opinion has the potential of becoming a solution to many slimy ore problems.

When ore and leach solution were run through the reactor no new problems were encountered. Ground chalcopyrite was leached in the reactor with 1N sulfuric acid. In this leach test the solid-liquid ratio was a function of the optimum rotation rate of the reactor (Figure 26). As the liquid-solid ratio decreased, the optimum rotational

speed increased. As the solid-liquid ratio becomes smaller the feed becomes more dense, thus resulting in more centrifugal force required to insure mixing.

When comparing the rotary tubular reactor with the other two types of reactors, the rotary tubular reactor excelled in the area of copper extraction. The copper extraction was chosen because of its slow rate constant and because the reaction was specifically dependent upon the mixing. The slimes in the ore could be seen (Figure 30) climbing up the sides of the constant stir tank and remaining unreacted. The rotary tubular reactor however increased the extraction of the copper by two and in some cases three times (Figure 27) as compared to extraction in the constant stir tank and plug flow models. The extraction of the copper was a function of the retention time in the reactor. Better extraction would occur if a longer residence time were used. In this case the experiment was not testing for the maximum copper extraction but comparing the rotary tubular reactor to other types of commercial reactors.

The previous work done by Jennings[12] was on a reactor similar to the one discussed in this paper. It is the closest work that the author has found to the rotary tubular reactor research. Jennings'[12] work was only for a one phase continuous system and the liquid RTD data presented was not specifically applicable to this system. The only curve generated from this data was a liquid pulse function curve. The present work goes much further toward defining the

mixing characteristics of the rotary tubular reactor. The solid-liquid step functions and the solid-liquid pulse functions are studied and defined for the reactor. Two different tracers were used for comparison showing that slimes and non-slime could both be handled by the reactor. The results generated from this paper show that the rotary tubular reactor has the potential of being a successful hydrometallurgical device. In the author's opinion the door has been opened to new research possibilities using the basic rotary tubular reactor design. More work must be done with a slimy tracer and step function curve data must be produced for the slimes. From such research the complete mixing characteristics of the slimes could be found. Other research work should include the study of the baffle size, baffle separation, and the length to diameter ratio so the optimum conditions for the reactor design may be found. Last but not least, various native slimy ores should be leached in the reactor so that the reactor may be predicted as to its feasibility for leaching all types of slimy ores commercially.

CONCLUSIONS

1. The rotary tubular reactor displays mixing characteristics unlike either the plug flow or back mix reactor designs. The mixing pattern generated contains the characteristics of both axial and radial mixing.

2. From the step function response curves the liquids and solids seem to exhibit similar RTD functions, a sign of good mixing. For the pulse RTD functions, the liquid and solid curves displayed a large amount of deviation from each other when the curves were simultaneously compared. In the author's opinion one reason for this deviation is the large liquid-solid ratio used in the experimentation.

3. The slimes show better axial mixing than the non-slimes in the reactor, displaying a higher dispersion (Peclet) number. The mixing characteristics of the slimes were similar to those of an ideal back mix reactor, thus alleviating the problem of the slimes adhering to the sides of the constant stir tank and remaining unreacted.

4. The experimental data show that the mixing in the rotary tubular reactor can be modeled as mixing in nine to ten constant stir tanks in series. It has also been predicted that the mixing from each cross section of baffles produce a flow pattern similar to that in a constant stir tank.

5. The rotary tubular reactor is capable of effectively handling solid-liquid ratios as small as 1:4.

6. Chalcopyrite can be leached with sulfuric acid in a rotary tubular reactor with a recovery of more than twice that obtained when the leaching takes place in a constant stir tank or a plug flow reactor.

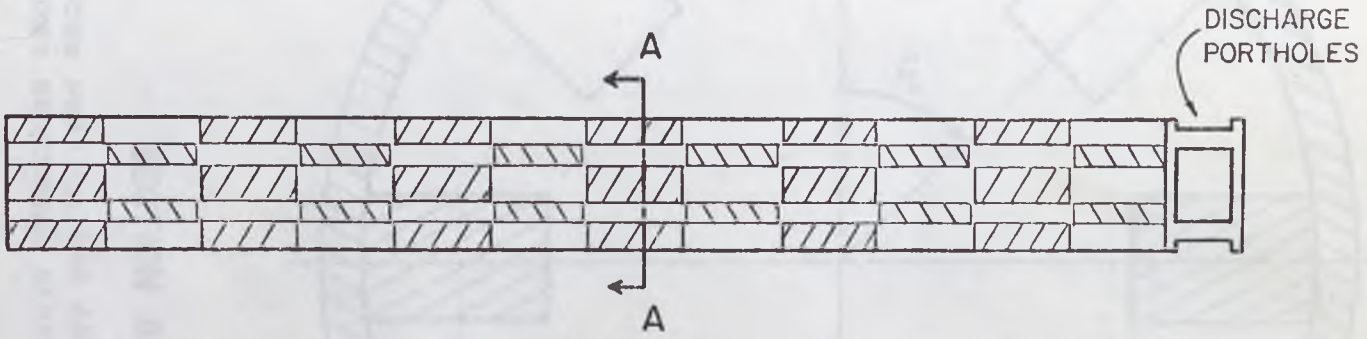

REACTOR TUBE SHOWING INTERNAL BAFFLES

Figure 8: Reactor tube showing internal baffles and discharge portholes. Reactor contains 44 baffles.

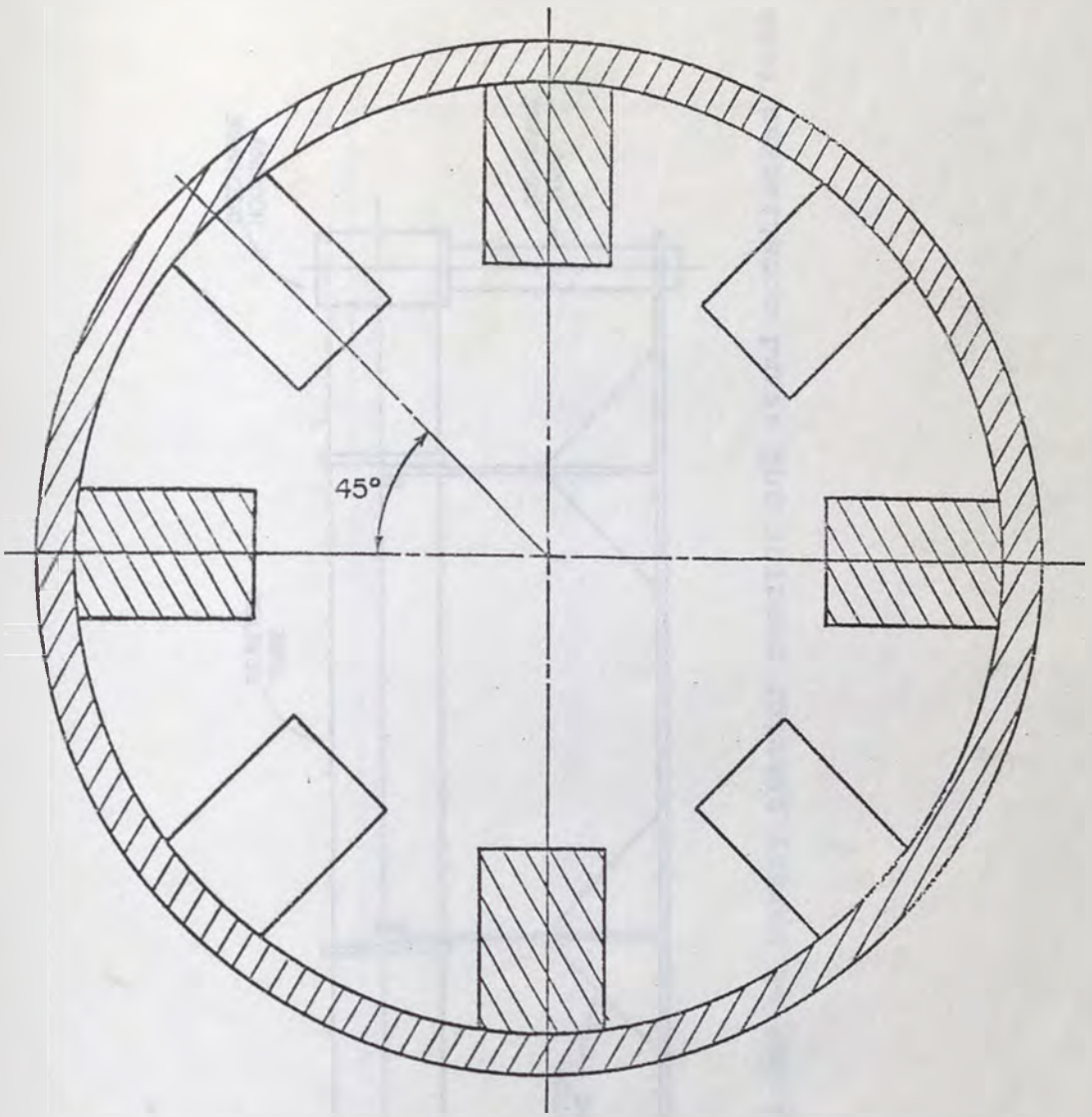

SECTION A-A

Figure 9: Cross section A-A showing the 4 baffles per cross sectional area.

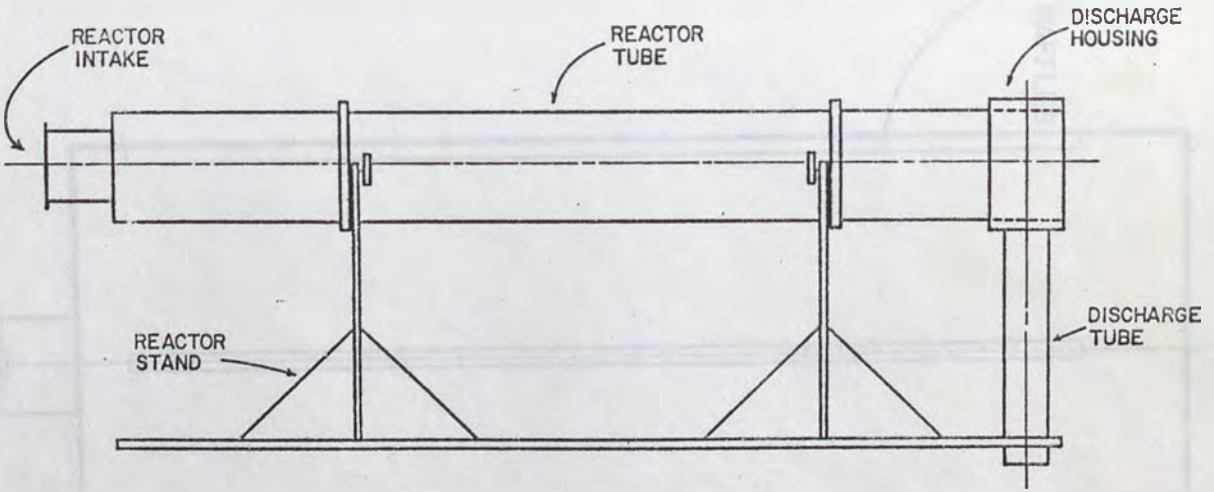

Figure 10: Schematic diagram of rotary tubular reactor and stand constructed from plexiglass.

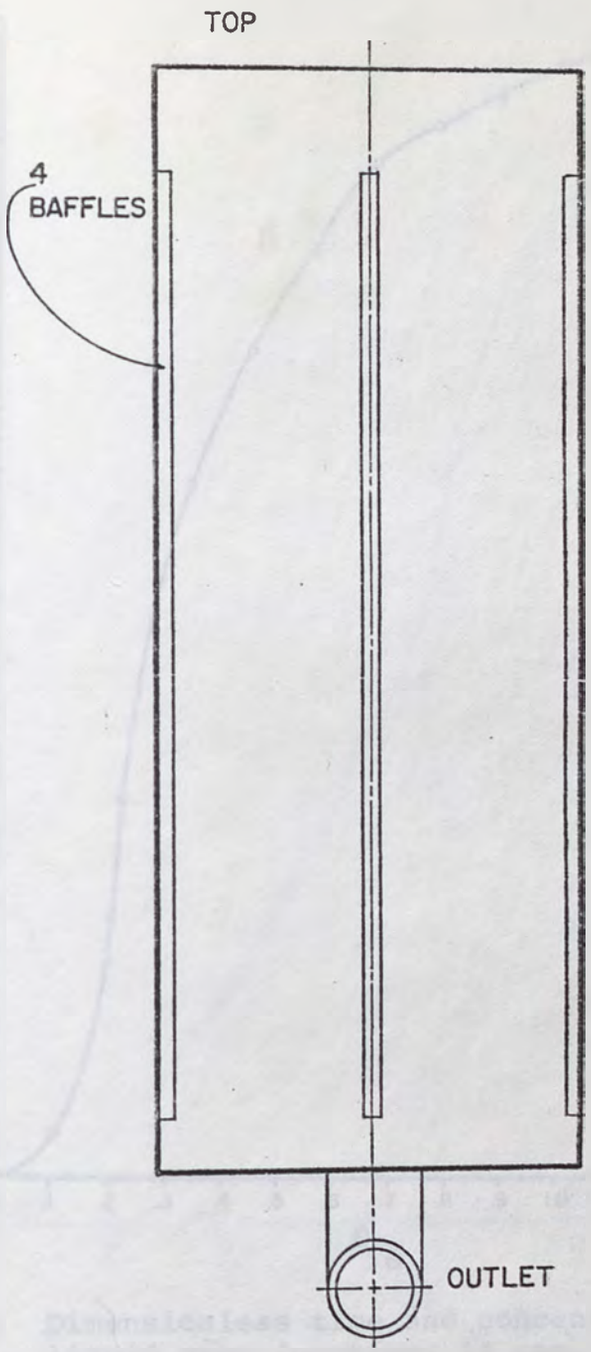

Figure 11: Schematic diagram of constant stir tank constructed from plexiglass and containing 4 longitudinal baffles.

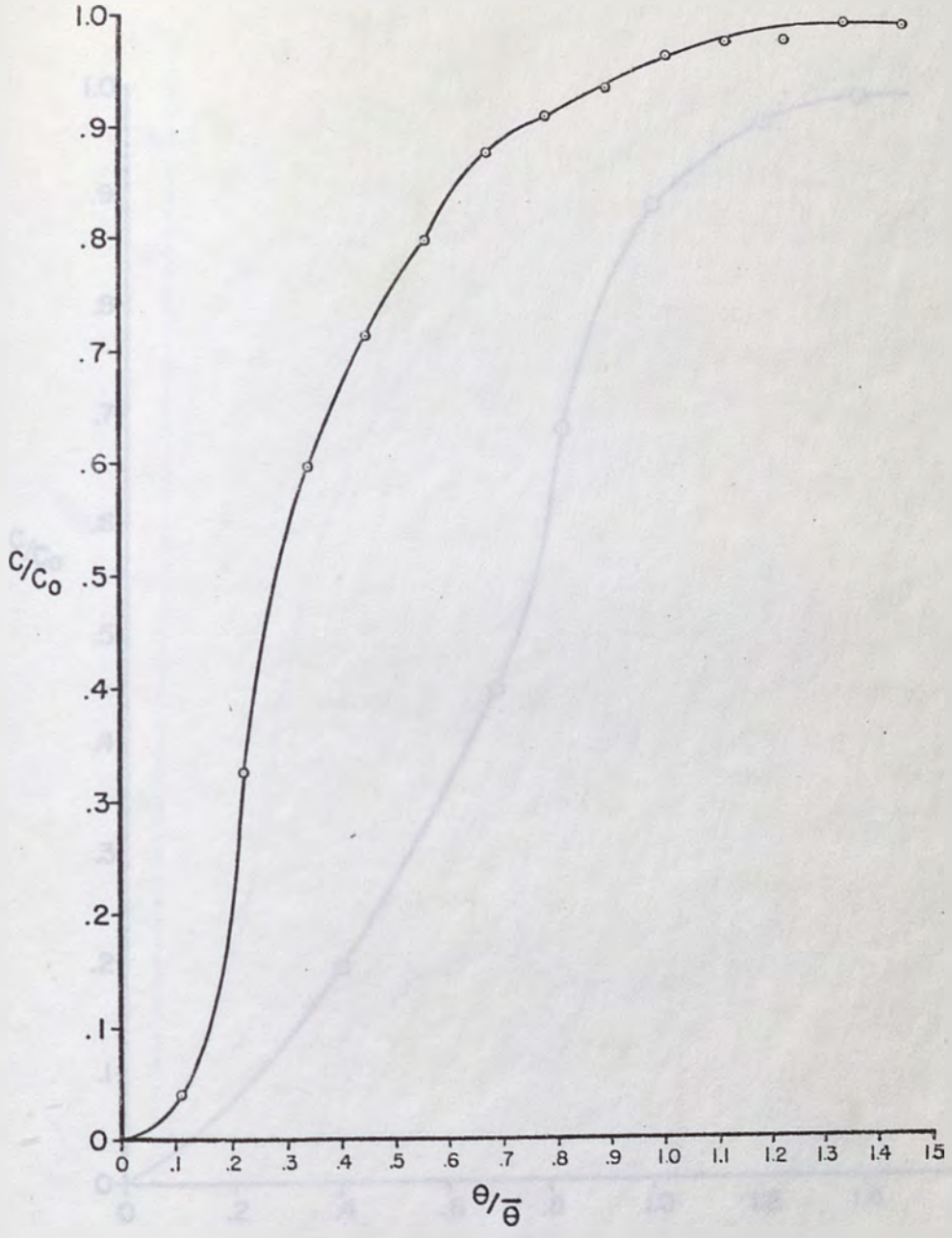

Figure 12: Dimensionless time and concentration plot of liquid step function, 14 rpm, 1:10 solid-liquid ratio.

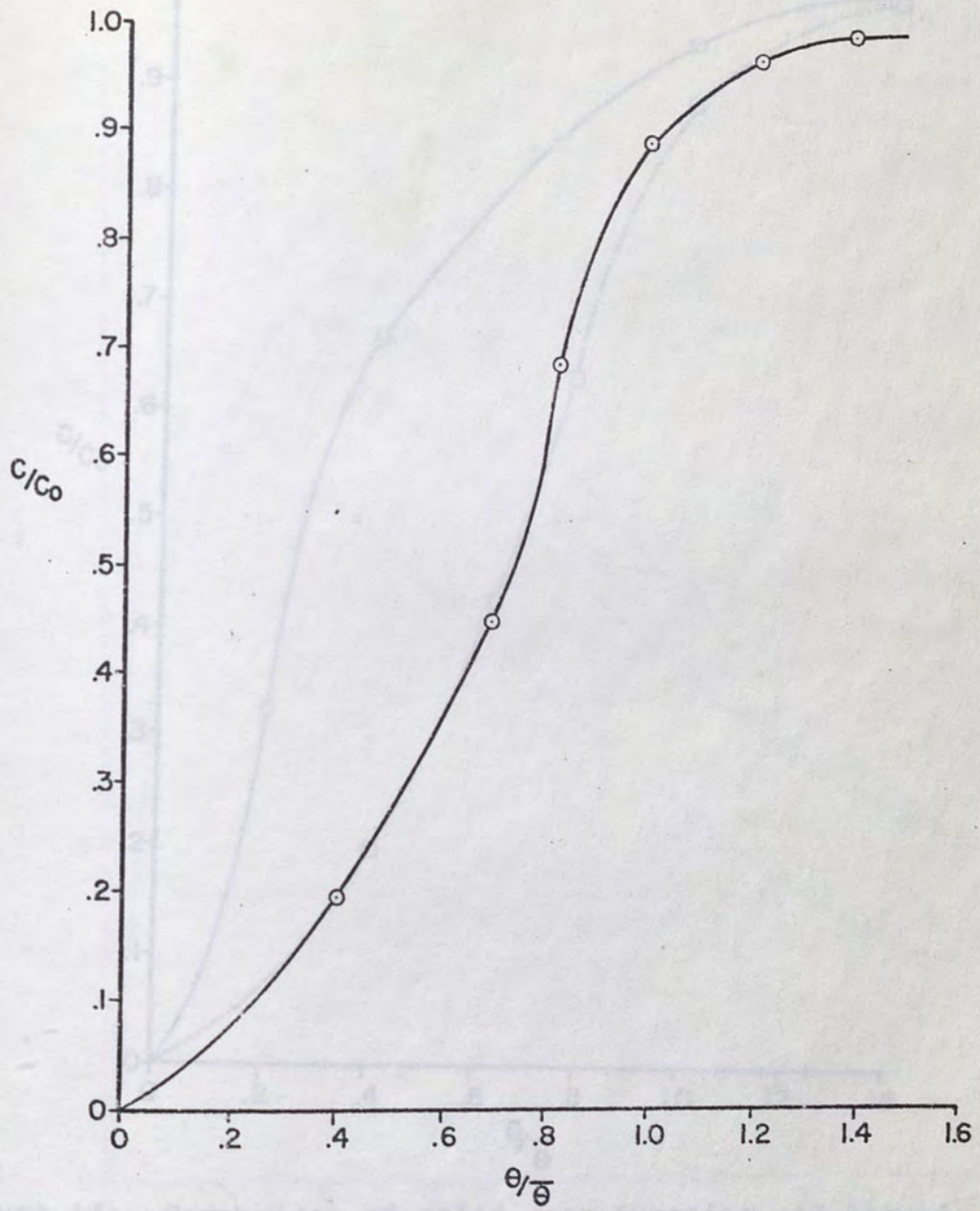

Figure 13: Dimensionless time and concentration plot of solids step function, 14 rpm, 1:10 solid-liquid ratio.

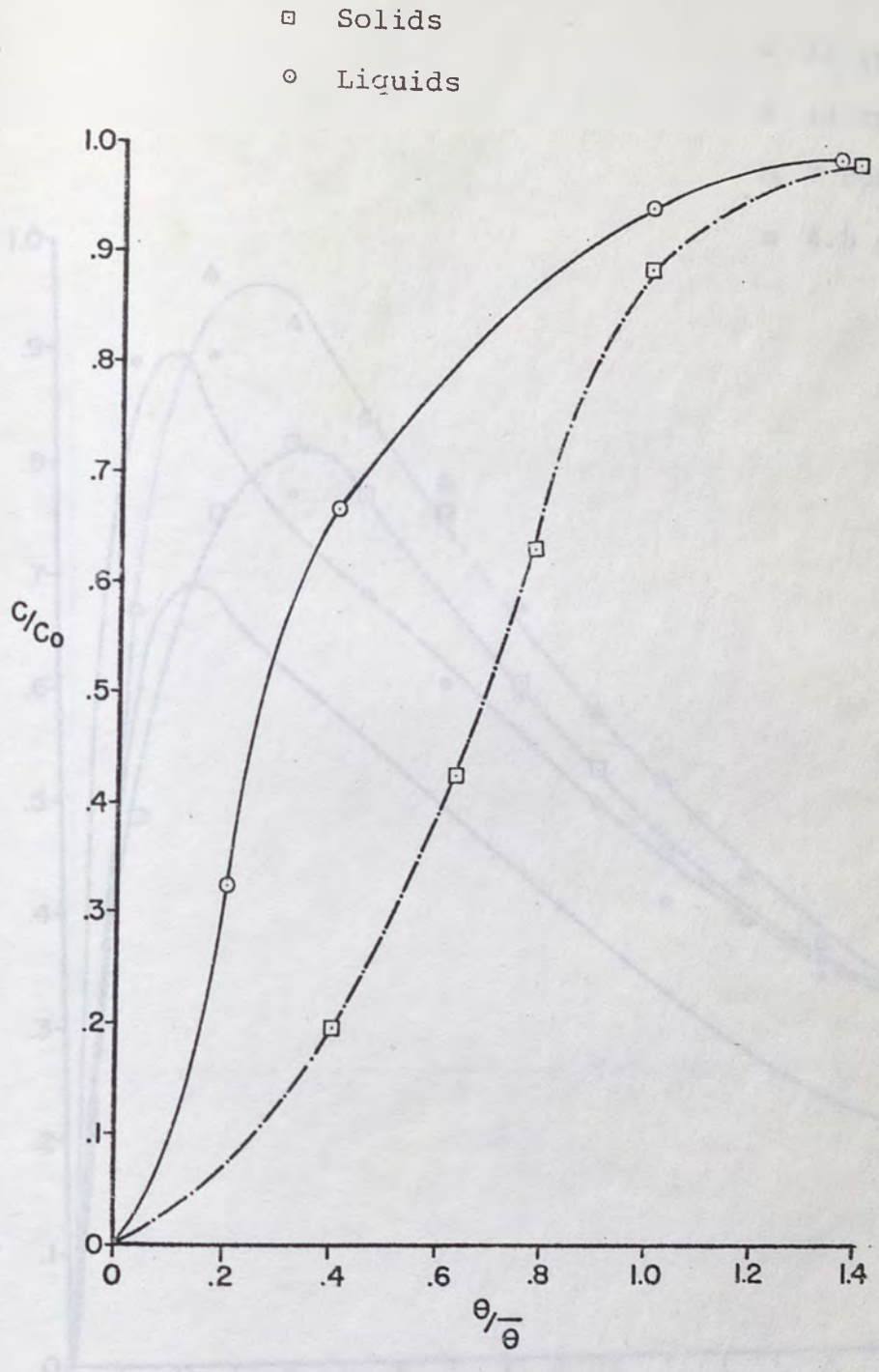

Figure 14: Comparison of solid step function and liquid step function, 14 rpm, 1:10 solid-liquid ratio.

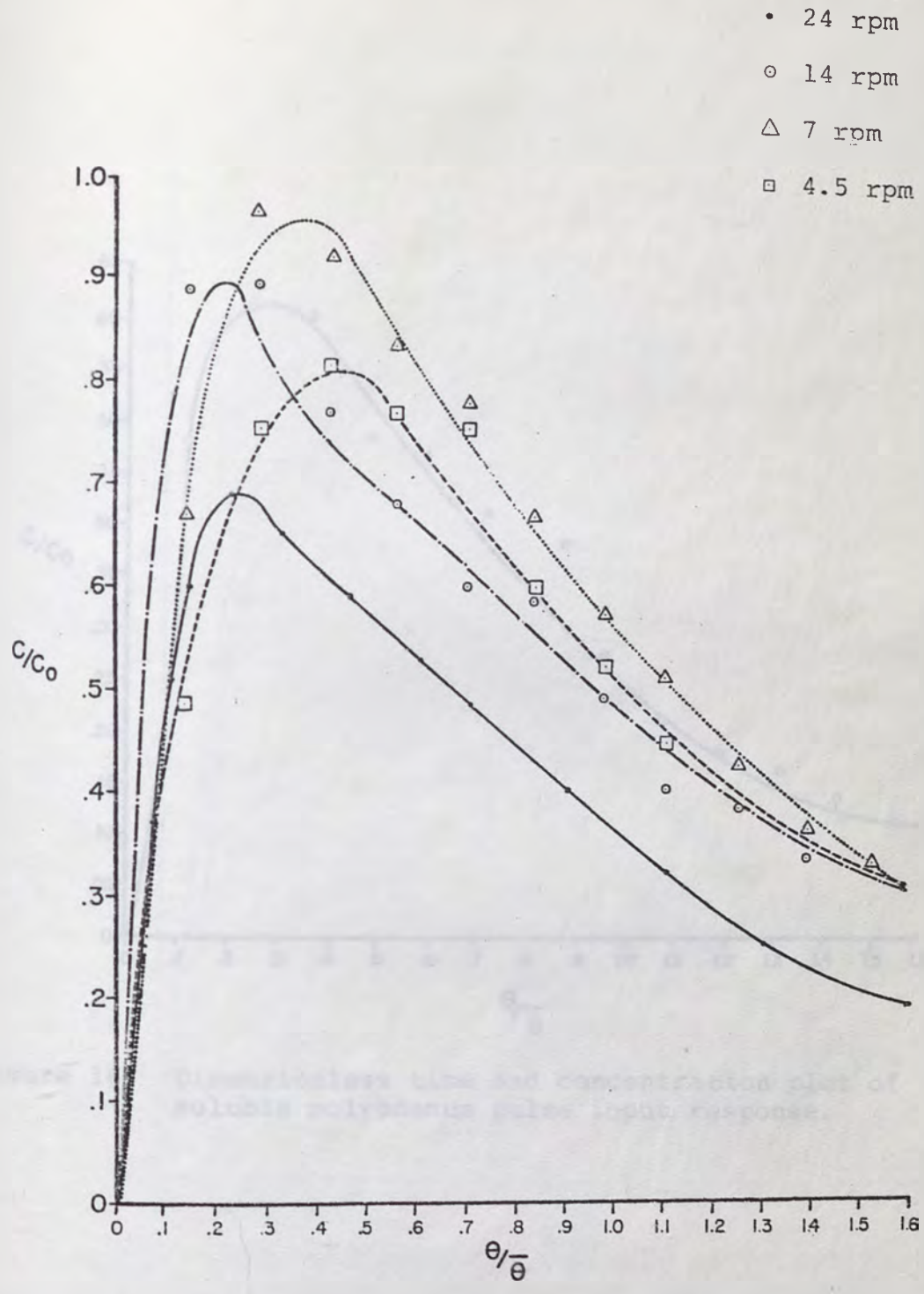

Figure 15: Dimensionless time and concentration plot of liquid pulse curves at various rotation rates. 1:10 solid-liquid ratio.

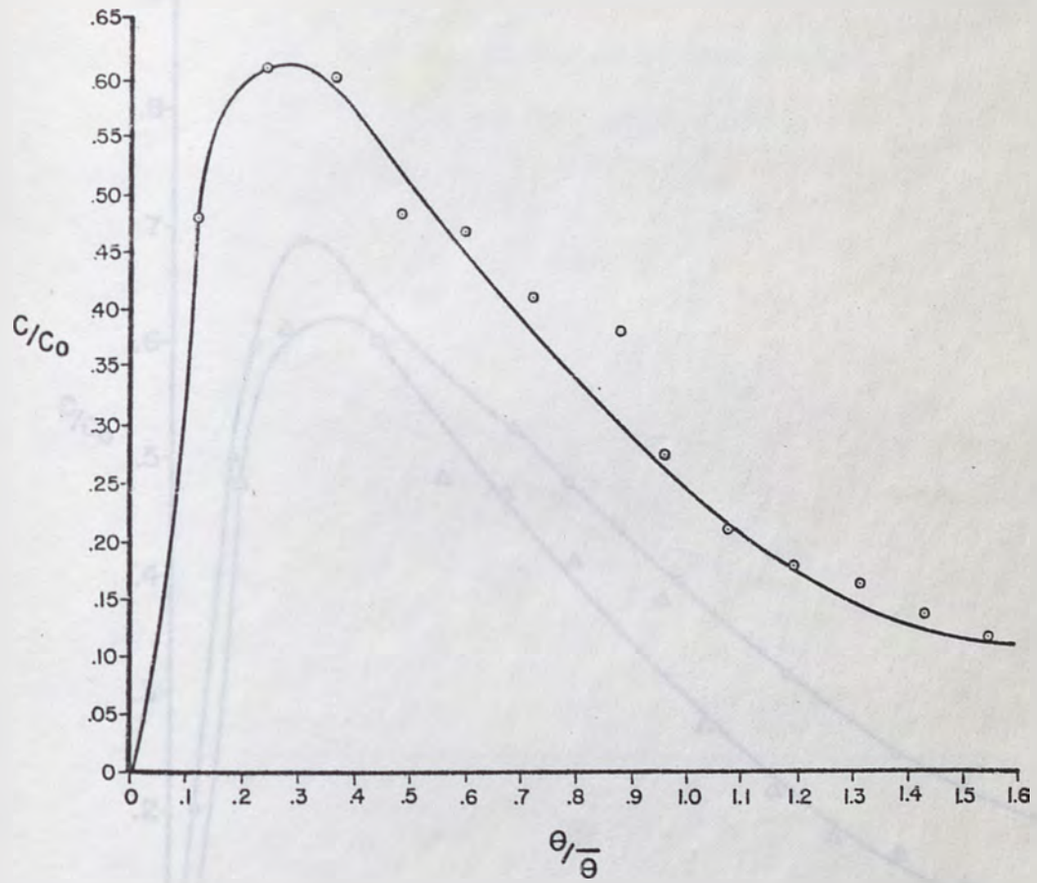

Figure 16: Dimensionless time and concentration plot of soluble molybdenum pulse input response.

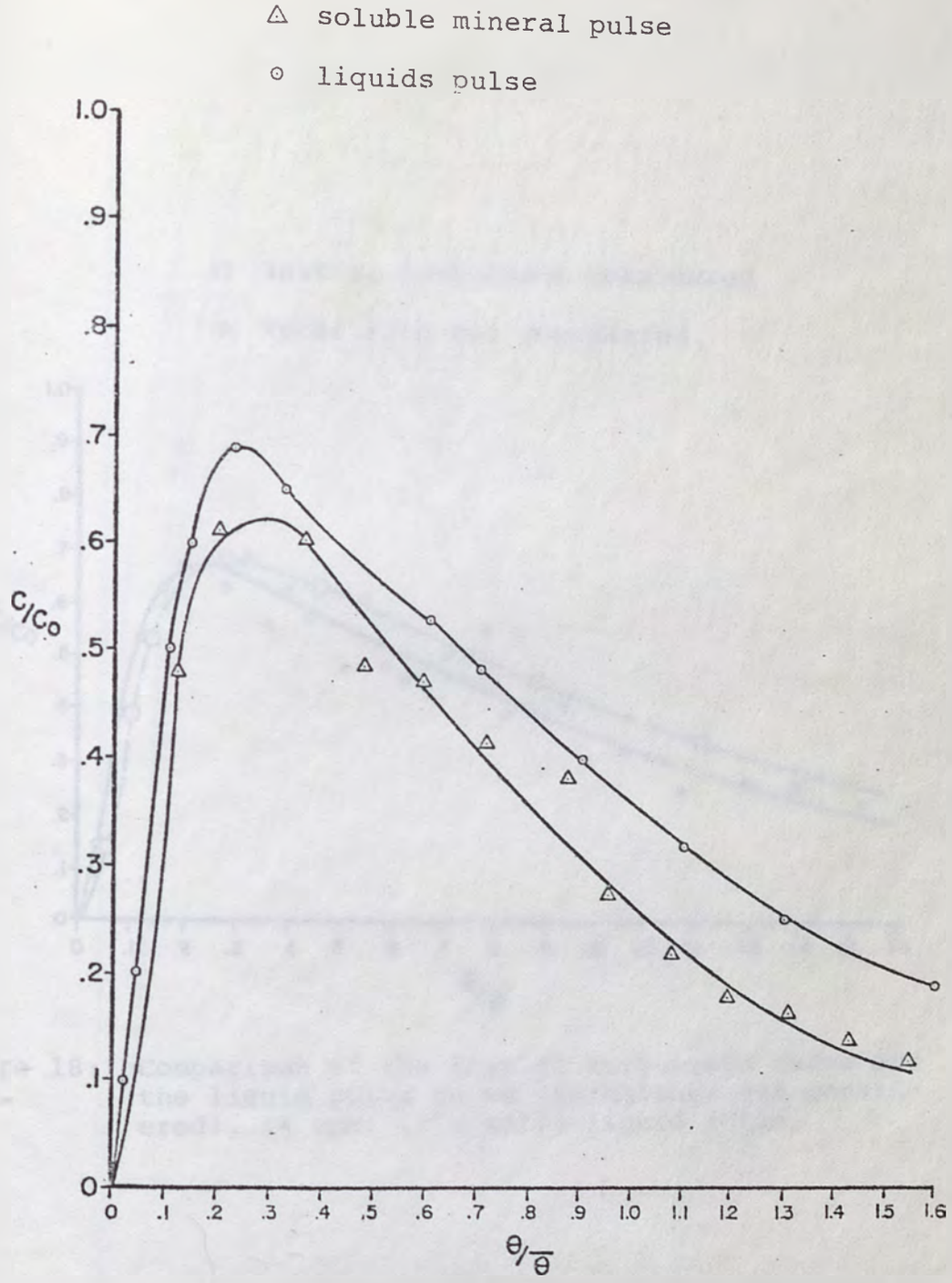

Figure 17: Comparison of 14 rpm liquid response curve and soluble molybdenum response curve, 1:10 liquid-solid ratio, 14 rpm.

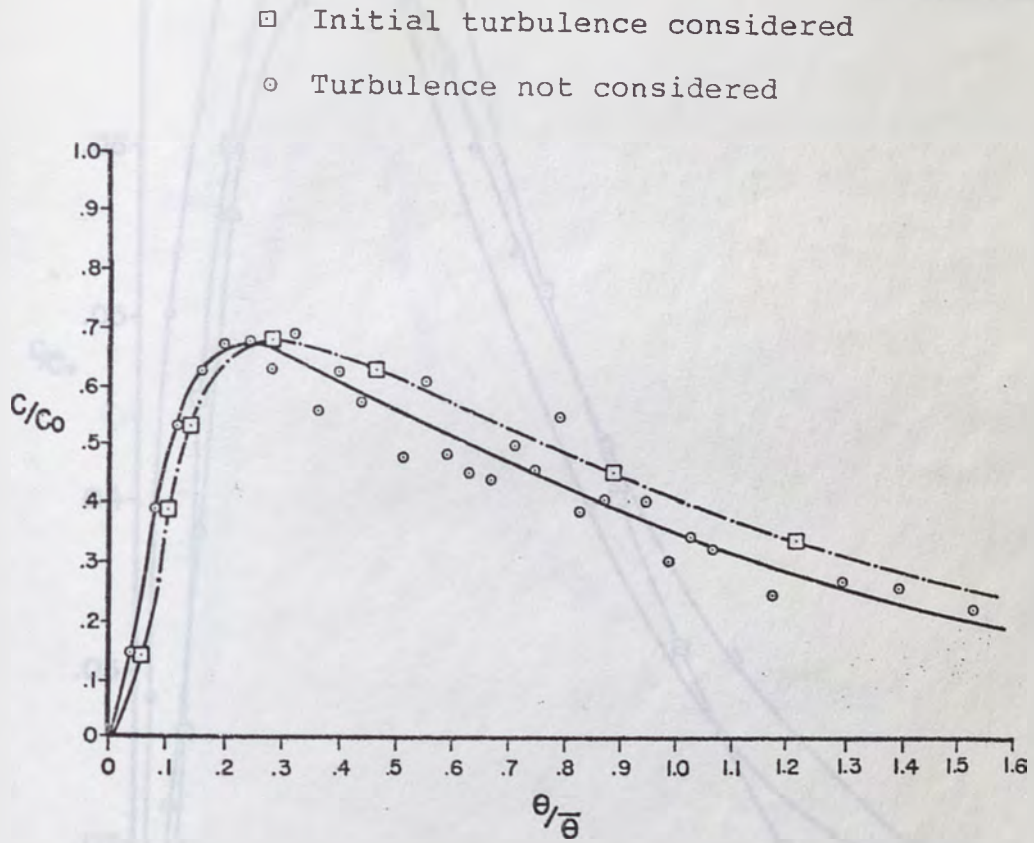

Figure 18: Comparison of the initial turbulence curve and the liquid pulse curve (turbulence not considered), 14 rpm, 1:10 solid-liquid ratio.

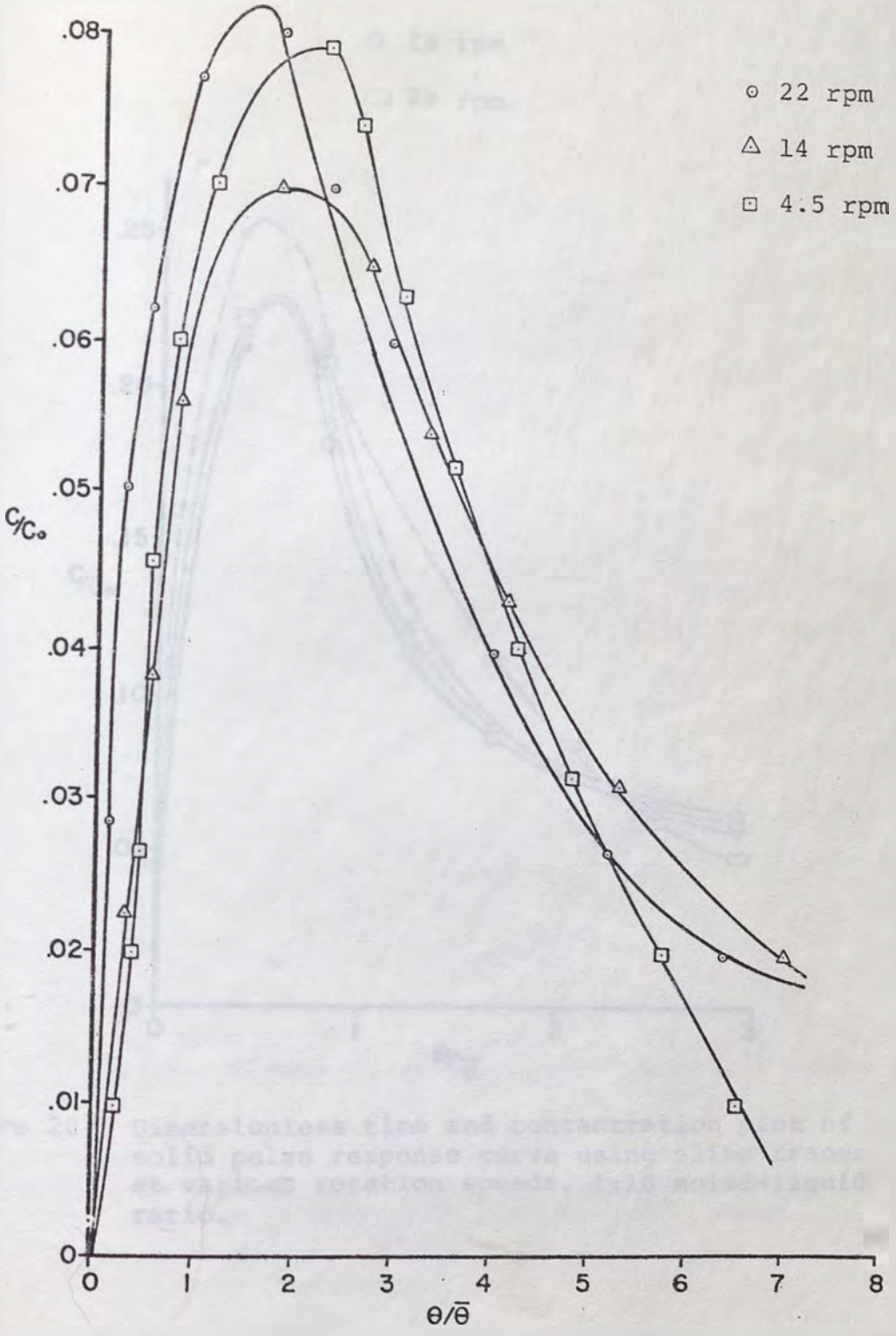

Figure 19: Dimensionless time and concentration plot of solid pulse response curve using non-slime tracer at various rotation speeds, 1:10 solid-liquid ratios.

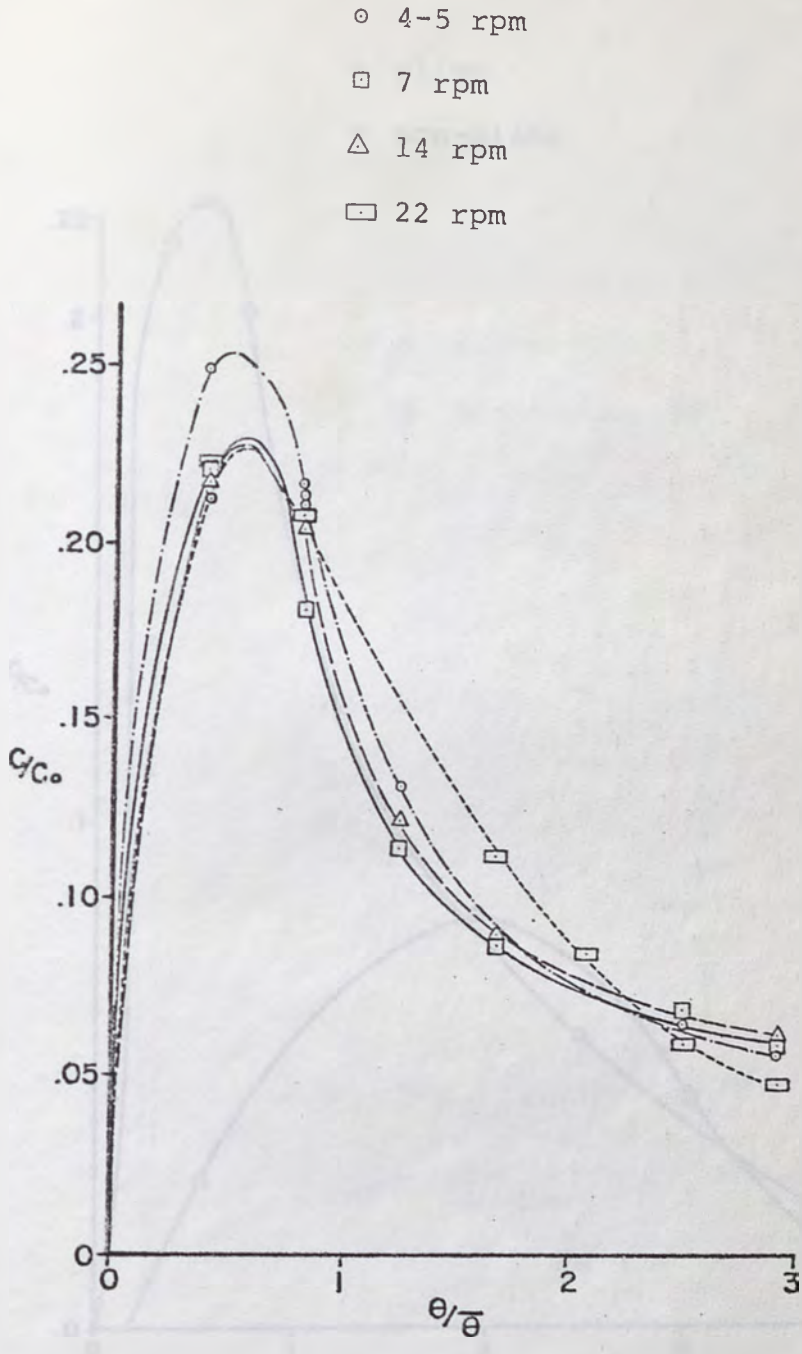

Figure 20: Dimensionless time and concentration plot of solid pulse response curve using slime tracer at various rotation speeds, 1:10 solid-liquid ratio.

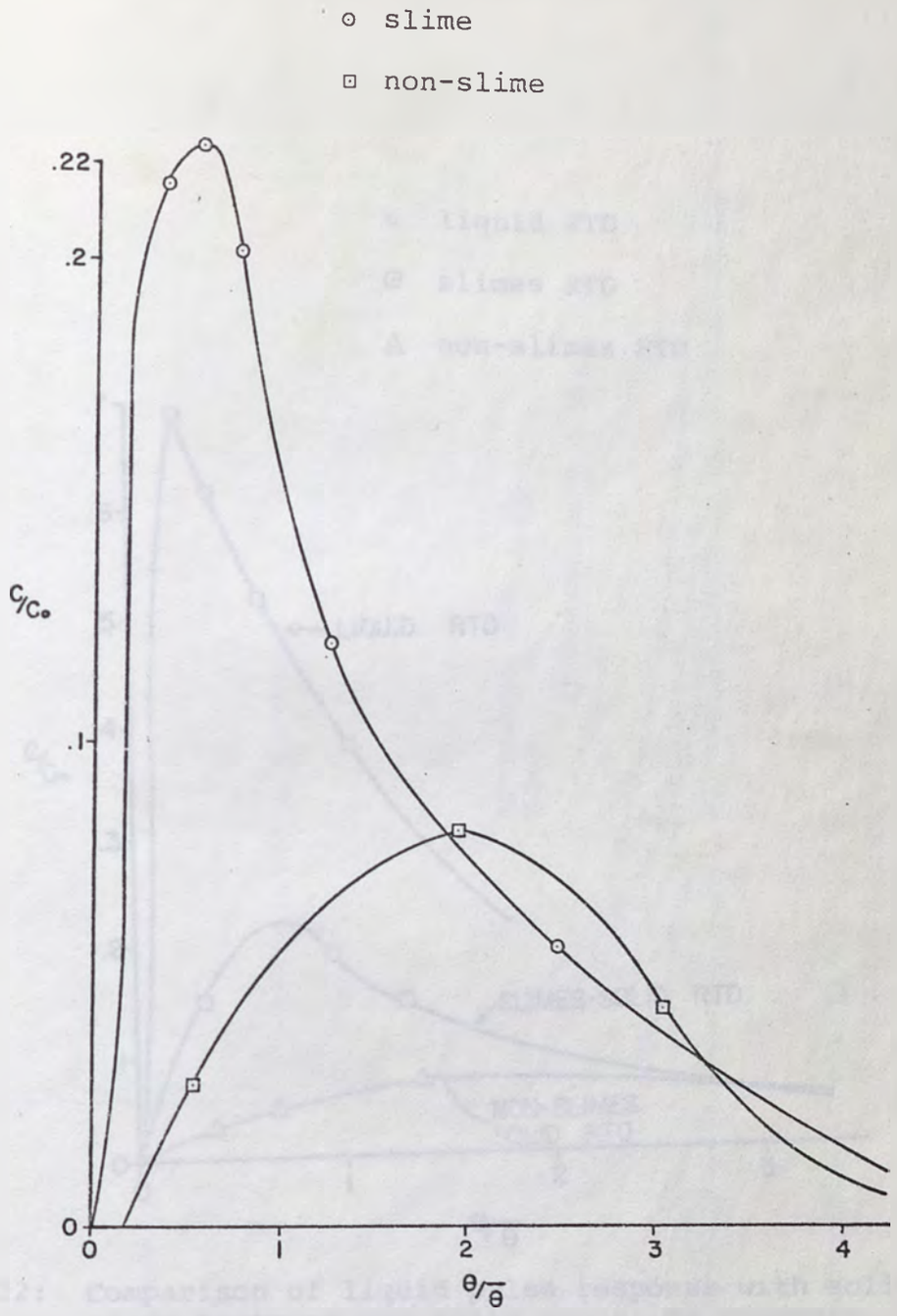

Figure 21: Comparison of slime and non-slime response curves, 14 rpm, 1:10 solid-liquid ratio.

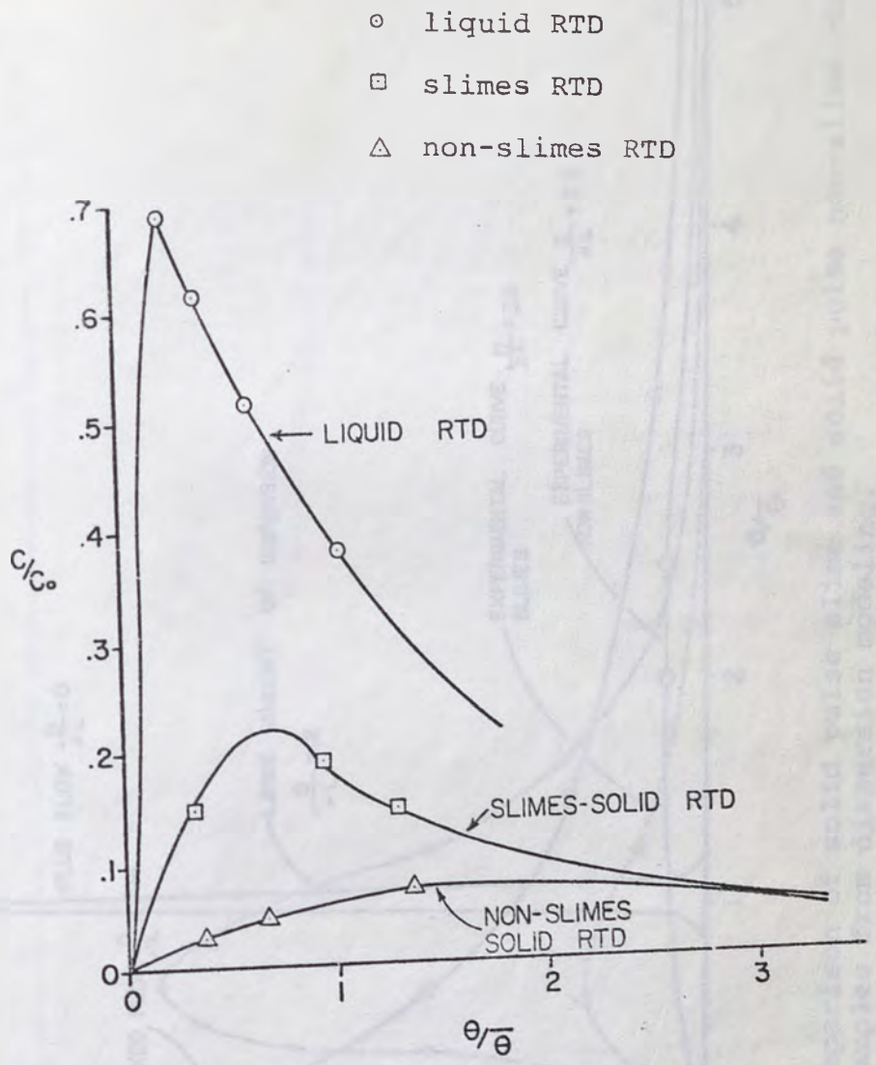

Figure 22: Comparison of liquid pulse response with solid slime response and solid non-slime response, 14 rpm, 1:10 solid-liquid ratio.

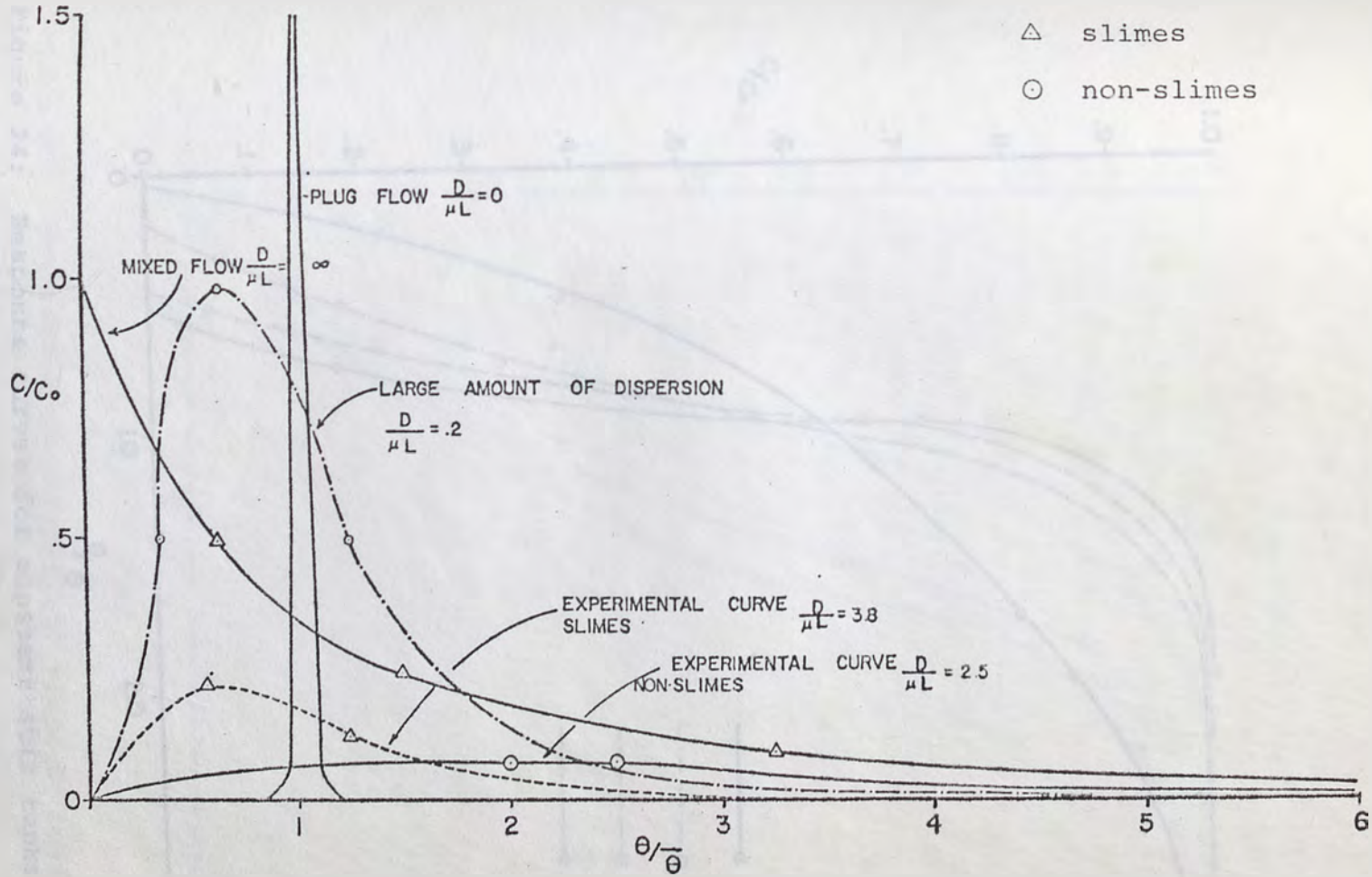

Figure 23: Comparison of solid pulse slime and solid pulse non-slime curves with examples from dispersion modeling.

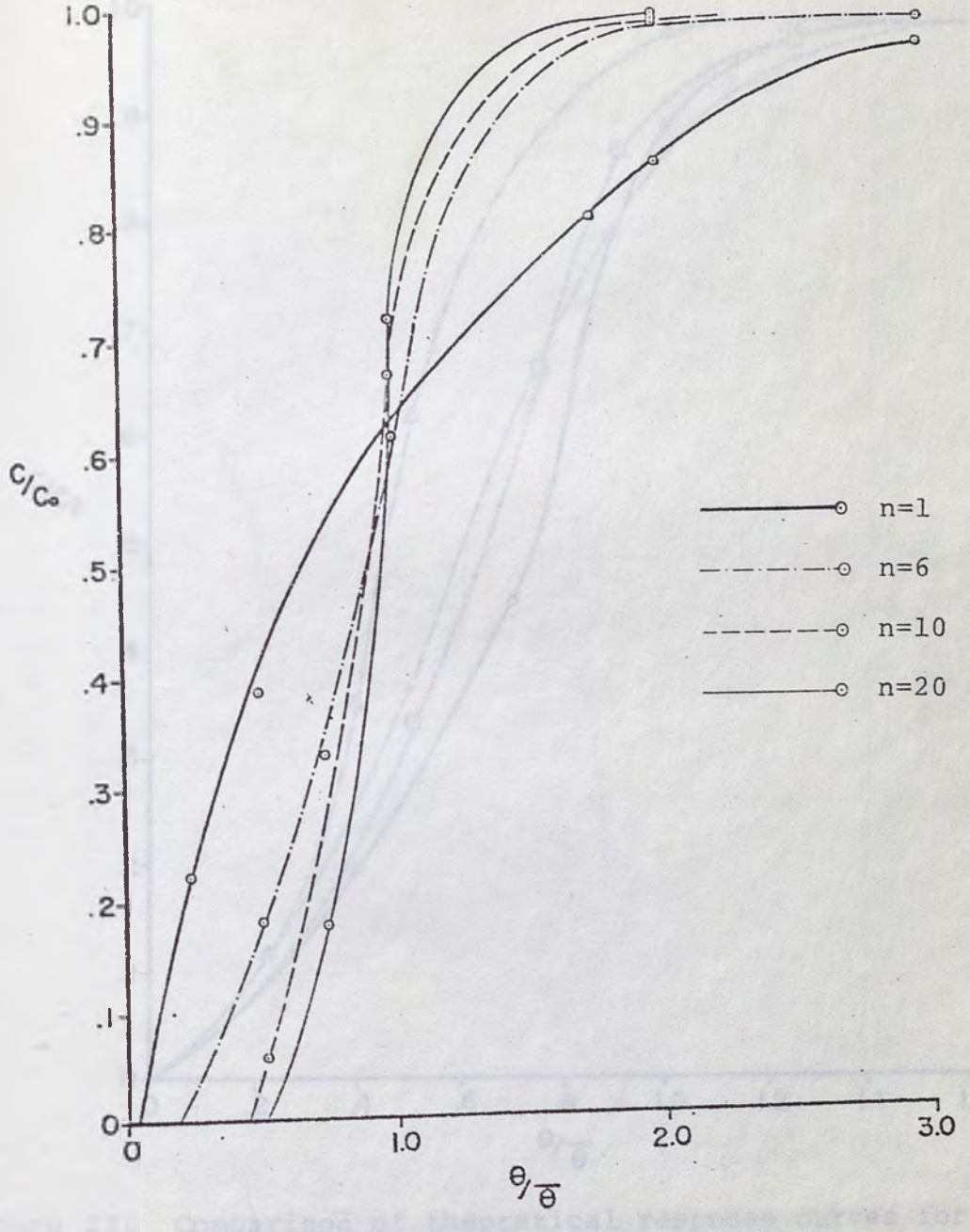

Figure 24: Response curves for constant stir tanks in series.

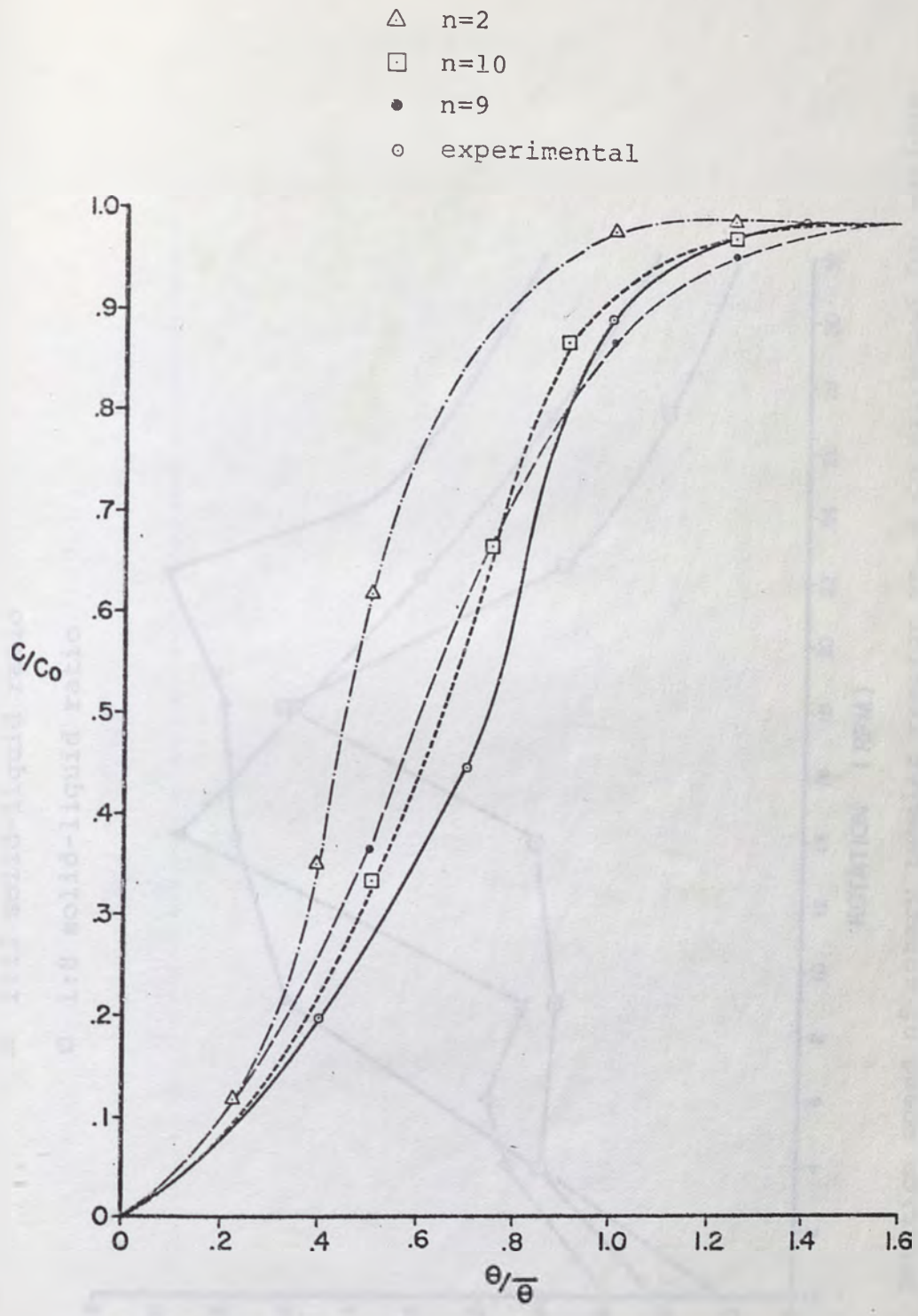

Figure 25: Comparison of theoretical response curves for constant stir tanks in series with the experimental solids step function curve.

⊙ 1:4 solid-liquid ratio

△ 1:13 solid-liquid ratio

⊡ 1:8 solid-liquid ratio

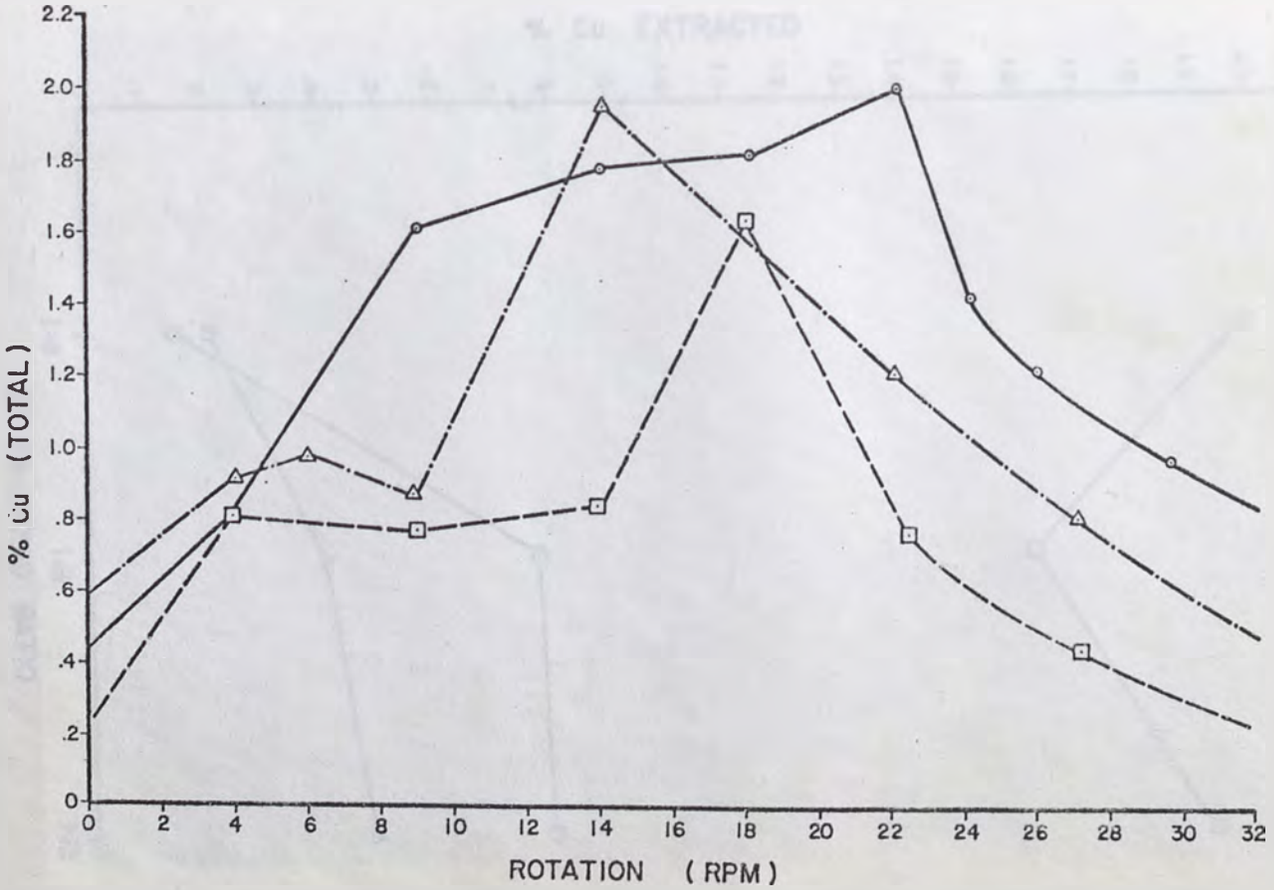

Figure 26: Rotation speed of rotary tubular reactor vs. % Cu extracted for various solid-liquid ratios.

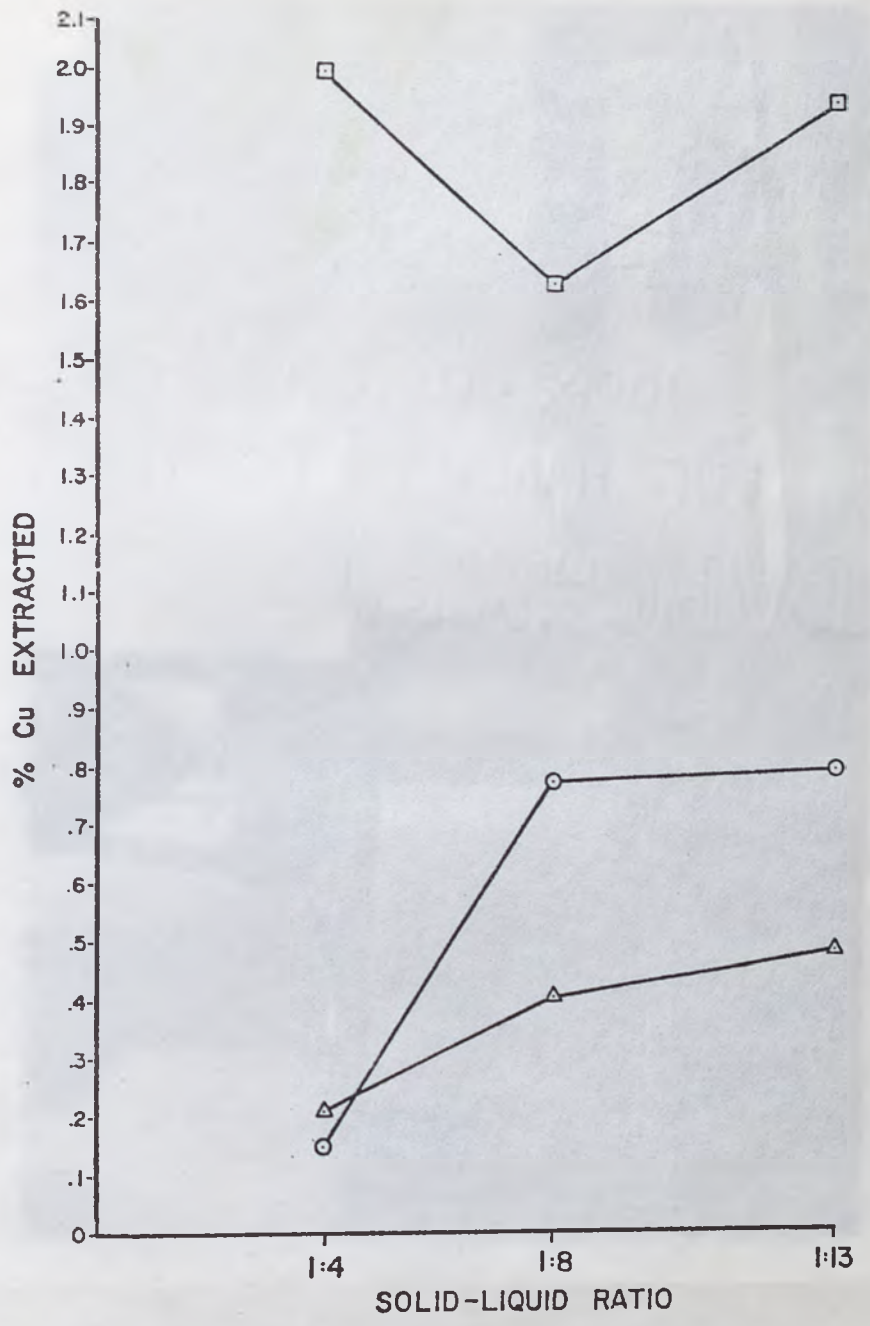

Figure 27: Solid-liquid ratio vs. % Cu extracted for the rotary tubular, plug flow, and constant stir tank reactor.

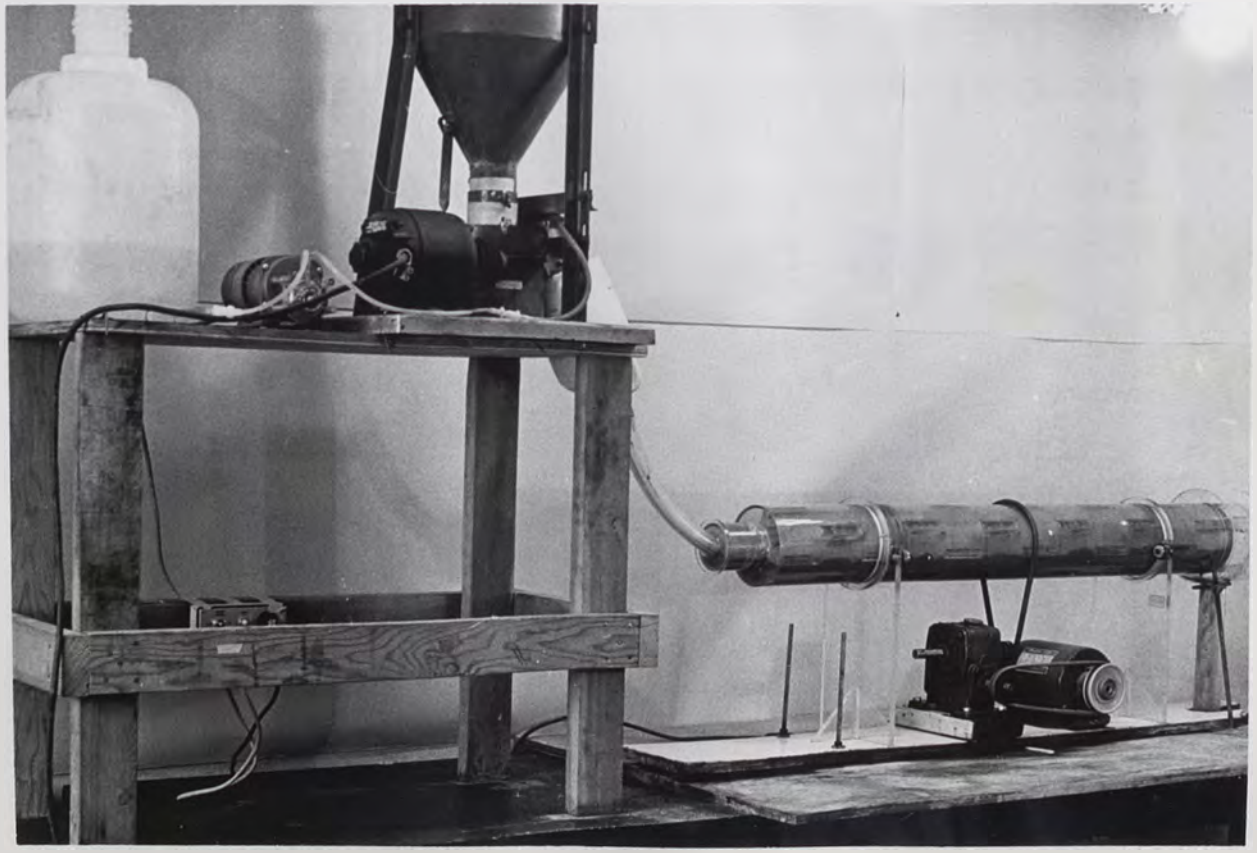

Figure 28: Rotary tubular reactor experimental set-up showing reactor, stand, and feed system.

Figure 29: Rotary tubular reactor in operation showing wave motion produced by baffles.

Figure 30: Slimes "climbing" up the sides of the experimental constant stir tank reactor.

Table I

Results of Sieve Tests on 0.5% Molybdenum "Salted" Ore

All Sieves: Tyler Series

Sample #1

Total Ore 949.10 g - 186.1 g = 763 g

Sieve	Total Wt. (g)	Sieve Wt. (g)	Sample Wt. (g)	Percent %	% Coarser
48	428.3	428.3	0	0	0
80	440.8	425.5	15.3	2	2
100	413.0	367.2	45.8	6	8
170	508.4	424.5	83.9	11	19
200	488.2	343.2	145.0	19	38
325	645.0	324.5	320.5	42	80
Pan	602.1	449.5	152.6	20	100

Sample #2

Total Ore 719.0 g - 186.1 g = 532.9 g

Sieve	Total Wt. (g)	Sieve Wt. (g)	Sample Wt. (g)	Percent %	% Coarser
48	428.3	428.3	0	0	0
80	436.2	425.5	10.7	2	2
100	415.2	367.2	48	9	11
170	467.1	424.5	42.6	8	19
200	460.4	343.2	117.2	22	41
325	553.6	324.5	229.1	43	84
Pan	534.8	449.5	85.3	16	100

Table II

Results of Sieve Test on 4.0% Copper "Salted" Ore

All Sieves - Tyler series

Total ore - 923.9 g - 186.1 g = 737.80 g

Sieve	Total Wt. (g)	Sieve Wt. (g)	Sample Wt. (g)	Percent %	% Coarser
48	428.3	428.3	0	0	0
80	469.8	425.5	44.3	6	6
100	382.0	367.2	14.8	2	8
170	564.4	424.2	140.2	19	27
200	461.2	343.2	118.0	16	43
325	619.6	324.5	295.1	40	83
Pan	574.9	449.5	125.4	17	100

Table III

Response Curve Data; Step Input; Fluids

1:10 solid:liquid ratio
14 rotations per minute

Time (min)	$\theta/\bar{\theta}$	C/C_o Run #1	C/C_o Run #2	C/C_o Run #3
0	0	0	0	0
5	0.111	0.035	0.048	0.042
10	0.222	0.273	0.378	0.326
15	0.333	0.551	0.648	0.600
20	0.444	0.677	0.752	0.715
25	0.555	0.798	0.809	0.804
30	0.666	0.857	0.901	0.879
35	0.777	0.909	0.912	0.911
40	0.888	0.945	0.934	0.940
45	1.000	0.970	0.967	0.969
50	1.111	0.997	0.967	0.982
55	1.222	1.000	1.000	1.000
60	1.333	0.998	1.000	0.999
65	1.444	1.000	1.000	1.000

Table IV

Response Curve Data; Step Input; Solids

1:10 solid-liquid ratio
14 rotations per minute

$\theta/\bar{\theta}$	C/C_o Run #1	C/C_o Run #2	C/C_o Run #3	C/C_o Run #4
0	0	0	0	0
0.119	0.074	0.075	0.750	0.075
0.238	0.530	0.150	0.175	0.126
0.357	0.251	0.150	0.110	0.170
0.467	0.356	0.208	0.225	0.263
0.595	0.357	0.352	0.350	0.353
0.714	0.374	0.400	0.411	0.395
0.833	0.649	0.660	0.659	0.656
0.952	0.808	0.860	0.873	0.847
1.070	0.900	0.895	0.897	0.897
1.190	0.925	0.916	0.919	0.920
1.250	0.978	0.974	0.979	0.977
1.310	0.996	0.990	0.998	0.994
1.420	0.999	1.00	0.999	1.00
1.540	0.999	0.999	1.00	1.00

Table V

Response Curve Data; Pulse Input; Liquids

1:10 solid-liquid ratio
14 rotations per minute

Time (min)	$\theta/\bar{\theta}$	C/C_o Run #1	C/C_o Run #2	C/C_o Run #3	C/C_o Run #4	Average C/C_o
2	0.039	0.036	0.429	0.029	0.091	0.1463
4	0.078	0.371	0.429	0.375	--	0.3917
6	0.118	0.393	0.571	0.546	0.625	0.5338
8	0.157	0.486	0.662	0.634	0.719	0.6253
10	0.196	0.657	0.700	0.654	--	0.6703
12	0.235	0.536	0.719	0.711	0.750	0.6790
14	0.275	0.536	0.662	0.671	--	0.6230
16	0.314	0.643	0.652	0.746	0.719	0.6900
18	0.353	0.443	0.643	0.600	--	0.5620
20	0.392	0.500	0.738	0.600	0.688	0.6315
22	0.431	0.443	0.710	0.571	--	0.5747
24	0.471	0.729	0.595	0.549	0.619	0.6230
26	0.510	0.371	0.548	0.546	--	0.4883
28	0.549	--	--	0.623	0.597	0.6100
30	0.588	0.429	0.476	0.537	--	0.4807
32	0.627	0.279	0.452	0.497	0.591	0.4548
34	0.667	0.321	0.542	0.457	--	0.4400
36	0.706	0.321	0.595	--	0.584	0.5000
38	0.745	0.321	0.619	0.449	--	0.4630
40	0.784	0.643	0.476	--	0.538	0.5533
42	0.824	0.357	--	0.423	--	0.3900
44	0.863	0.357	0.329	--	0.531	0.4057
46	0.902	0.386	0.542	0.414	--	0.4473
48	0.941	0.321	0.376	--	0.525	0.4073
50	0.980	0.229	0.286	0.394	--	0.3030
52	1.02	0.214	--	--	0.469	0.3415
54	1.06	0.286	--	0.366	--	0.3260
56	1.098		--	--	--	
58	1.137		--	--	--	
60	1.176		0.190	0.291		0.2405
62	1.216			--	--	
64	1.255			--	--	
66	1.294			0.271	0.272	0.2715
68	1.333			--		
70	1.373			--		
72	1.393			0.257		0.257
74	1.451			--		
76	1.490			--		
78	1.529			0.223		0.223
80						

Table VI

Response Curve Data; Pulse Input; Liquids

1:10 Solid-liquid ratio

Time (min)	$\theta/\bar{\theta}$	C/C_o 24rpm	C/C_o 4.5rpm	C/C_o 7rpm	C/C_o 14rpm
0	0	0	0	0	0
5	0.139	0.886	0.486	0.667	
10	0.278	0.892	0.754	0.963	
15	0.417	0.769	0.815	0.919	Data
20	0.556	0.677	0.769	0.833	taken
25	0.694	0.600	0.754	0.770	from
30	0.833	0.585	0.600	0.667	14rpm
35	0.972	0.492	0.523	0.574	Ave.
40	1.111	0.400	0.446	0.511	(Table V)
45	1.250	0.385	--	0.426	
50	1.389	0.335	0.388	0.363	
55	1.528	0.338	--	0.333	
60	1.667	0.246	--	0.378	
65	1.806	0.262	--	0.241	
70	1.944	0.215	--	--	
75					

Table VII

Response Curve Data; Pulse Curve; Soluble Molybdenum

1:10 solid-liquid ratio
14 rotations per minute

Time (min)	$\theta/\bar{\theta}$	C/C_o Run #1	C/C_o Run #2	Average C/C_o
0	0	0	0	0
5	0.119	0.667	0.229	0.448
10	0.238	0.963	0.257	0.610
15	0.357	0.919	0.291	0.605
20	0.476	0.833	0.139	0.486
25	0.595	0.770	0.171	0.471
30	0.714	0.667	0.163	0.415
35	0.875	0.574	0.171	0.373
40	0.952	0.511	0.042	0.277
45	1.071	0.426	--	0.213
50	1.190	0.363	--	0.182
55	1.310	0.333	--	0.167
60	1.429	0.278	--	0.139
65	1.548	0.241	--	0.121

Table VIII

Response Curve Calculations for Consideration of Initial Turbulence in the Rotary Tubular Reactor

Initial turbulence not considered
14 rotations per minute
1:10 solid-liquid ratio

$\theta/\bar{\theta}$	C/C_o
0.000	0.000
0.039	0.146
0.118	0.634
0.196	0.670
0.275	0.623
0.353	0.562
0.431	0.575
0.510	0.486
0.588	0.481
0.667	0.440
0.745	0.463
0.824	0.390
0.902	0.447
0.980	0.303
1.060	0.326
1.176	0.241
1.294	0.272
1.393	0.257

Initial turbulence considered
14 rotations per minute
1:10 solid-liquid ratio

$\theta/\bar{\theta}$	C/C_o
0	0.000
0.116	0.412
0.233	0.676
0.349	0.666
0.465	0.622
0.581	0.591
0.698	0.542
0.814	0.443
0.930	0.422
1.050	0.418
1.160	0.361
1.280	0.340
1.400	0.310
1.510	0.270

Table IX

Response Curve Data, Pulse Input, Solids;
Thorite Tracer 100% + 100 Mesh

1:10 solid-liquid ratio

$\theta/\bar{\theta}$	C/C_o 14rpm	C/C_o 4.5rpm	C/C_o 22rpm
0.294	0.022	0.018	0.055
0.588	0.062	0.049	0.062
0.882	0.075	0.061	0.074
1.180	0.073	0.064	0.080
1.470	0.065	0.074	0.082
1.760	0.073	0.076	0.079
2.060	0.064	0.078	0.073
2.350	0.062	0.078	0.065
2.640	0.047	0.076	0.062
2.940	0.062	0.074	0.058
3.230	0.037	0.067	0.054
3.530	0.051	0.059	0.045
3.820	0.051	0.052	0.043
4.120	0.043	0.045	0.039
4.410	0.043	0.043	0.035
4.710	0.029	0.043	0.032
5.000	0.027	0.032	0.030
5.290	0.031	0.028	0.024
5.590	0.023	0.023	0.023
5.880	0.030	0.020	0.022
6.170	0.021	0.016	0.021
6.470	0.024	0.012	0.021
6.670	0.009	0.010	0.020

Table X

Response Curve Data; Pulse Input; Solids
Pitchblend Tracer 100% - 325 Mesh

1:10 solid-liquid ratio

$\theta/\bar{\theta}$	C/C_o 22rpm	C/C_o 4.5rpm	C/C_o 7rpm	C/C_o 14rpm
0	0	0	0	0
0.417	0.210	0.249	0.218	0.209
0.833	0.207	0.210	0.183	0.208
1.250	0.114	0.131	0.129	0.114
1.667	0.107	0.079	0.090	0.080
2.083	0.105	0.084	0.075	0.083
2.500	0.060	0.066	0.071	0.068
2.920	0.048	0.056	0.058	0.056
3.330	0.034	0.052	0.049	0.050
3.750	0.061	0.039	0.034	0.034
4.167	0.019	0.019	0.031	0.024
4.580	0.013	0.011	0.023	0.016
5.000	0.010	0.005	0.015	0.009
5.410	0.006	0.004	0.011	0.008
5.830	0.003	0.002	0.007	0.003

Table XIa

Data for Calculation of Peclet Number by Variance Method
For Non-slime Pulse Curve

14 rotations per minute

t (min)	C_i counts/min	t_iC_i	$t_i^2C_i$
15	2223	33345	500175
30	4592	137760	4132800
45	5106	229770	10339650
60	5745	344700	15511500
75	4891	366825	27511875
90	5070	456300	41067000
105	4195	440475	46249875
120	4652	558240	66988800
135	3497	472095	63732825
150	5755	863250	129487500
165	3559	587235	96893775
180	5625	1012500	182250000
195	3721	725595	141491025
210	5246	1101660	231348600
225	2681	603225	135725625
240	2562	614880	147571200
255	3180	810900	20677950
270	1984	535680	144633600
285	3195	910575	259513875
300	1431	429300	128790000
315	3117	981855	309284325
330	2812	927960	306226800
345	2400	828000	285660000
360	1900	684000	346240000
375	1000	375000	140625000
390	221	86190	33614100

Table XIb

Data for Calculating Peclet Number by Variance Method
For Slimy Pulse Curve

14 rotations per minute

t (min)	C_i counts/min	t_iC_i	$t_i^2C_i$
15	5733	86000	129000
30	4821	144600	4339000
45	3382	152000	6849000
60	2357	141420	8485000
75	1966	147450	11058750
90	1862	167580	15082200
105	1520	159600	16758000
120	1288	154560	18547200
135	899	121365	16384275
150	800	120000	18000000
165	600	99000	16335000
180	400	72000	12960000
195	300	58500	11407500
210	200	42000	8820000
225	100	22500	5062500

Table XII

Results of Chalcopyrite-Sulfuric Acid Leach on Three Types of Reactors

Ore Assay - 4.0% Total Cu

RPM	% Cu Extracted
1:13 SOLID-LIQUID RATIO	
4	0.91
6	0.98
9	0.94
14	1.95
18	1.56
22	1.21
CSTR*	0.81
Plug Flow	0.59
1:8 SOLID-LIQUID RATIO	
4	0.82
6	--
9	0.77
14	0.84
18	1.64
22	0.80
24	--
CSTR*	0.77
Plug Flow	0.44
1:4 SOLID-LIQUID RATIO	
9	1.61
14	1.80
18	1.82
22	2.00
24	1.41
CSTR*	0.18
Plug Flow	0.23

*CSTR = Constant Stir Tank Reactor

APPENDIX I

Equations and Calculations for Dispersion (Peclet) Numbers

a) For non-Slimes

From Table XIa the following may be found:

$\bar{t}$ = 51 min

ΣC_i = 90360

$\Sigma t_i C_i$ = 15117315

$\Sigma t_i^2 C_i$ = 3282770125

Following procedure as stated in theory:

$\sigma^2 = 36329.9 - (167.30)^2$

$\sigma^2 = 8340$

$\sigma^2 = \sigma^2/\bar{t}^2 = 3.21$

$$3.21 = 2\frac{D}{\mu L} - \left[2\frac{D}{\mu L}(1 - e^{-\mu L/D})\right]$$

by approximating

$$\frac{D}{\mu L} = 3.8$$

b) For Slimes

From Table XIb the following may be found:

$\bar{t}$ = 26.6 min

ΣC_i = 26230

$\Sigma t_i C_i$ = 1688575

$\Sigma t_i^2 C_i$ = 170217425

Following procedure as stated in theory:

$\sigma^2 = 6489 - (64.37)^2$

$\sigma^2 = 2345$

$\sigma^2 = \sigma^2/\bar{t}^2 = 5.86$

$$5.86 = 2\frac{D}{\mu L} - [2\frac{D}{\mu L}(1 - e^{-\mu L/D})]$$

by approximating

$$\frac{D}{\mu L} = 3.8$$

APPENDIX II

Computer Program Used for Computing Numbers Needed to Plot Figure 24, (n-constant Stir Tanks in Series)

```
76/04/21. 10.03.13.
UNIV OF NEVADA TIME SHARING SYSTEM.    KRONOS 2.1 397
USER NUMBER:  BEB3A16,HUEFTLE
PASSWORD

TERMINAL:      34,TTY
RECOVER /SYSTEM:FORTRAN
OLD, NEW, OR LIB FILE:  OLD,TEST
READY.

LNH

00050     PROGRAM KENT(INPUT,OUTPUT)
00100  40 READ,Y
00110     DO 10 N=1,20
00120     SUM=0
00125     E=2.71828
00130     K=N-1
00135     TERM=1.
00140     DO 20 I=1,K
00145    SUM=SUM+TERM
00150  20 TERM=N*Y*TERM/I
00180     X=1-(E**((-N)*Y)*SUM)
00190    PRINT 30,Y,N,X
00200  30 FORMAT(*FOR Y = *,F4.2,* AND N = *,I2,* X = *,F6.4)
00210  10 CONTINUE
00215     GO TO 40
00220     STOP
00230     END
READY.

RNH
```

```
  002124B     215. 00220    STOP
 SEQ   230. CAUTION - STATEMENT CANNOT BE EXECUTED -
                     NO STATEMENT NUMB
? .1
FOR Y =  .10    AND     N =  1 X =     .0952
FOR Y =  .10    AND     N =  2 X =     .1813
FOR Y =  .10    AND     N =  3 X =     .0369
FOR Y =  .10    AND     N =  4 X =     .0079
FOR Y =  .10    AND     N =  5 X =     .0018
FOR Y =  .10    AND     N =  6 X =     .0004
FOR Y =  .10    AND     N =  7 X =     .0001
FOR Y =  .10    AND     N =  8 X =     .0000
FOR Y =  .10    AND     N =  9 X =     .0000
FOR Y =  .10    AND     N = 10 X =     .0000
FOR Y =  .10    AND     N = 11 X =    -.0000
FOR Y =  .10    AND     N = 12 X =    -.0000
FOR Y =  .10    AND     N = 13 X =    -.0000
FOR Y =  .10    AND     N = 14 X =    -.0000
FOR Y =  .10    AND     N = 15 X =    -.0000
FOR Y =  .10    AND     N = 16 X =    -.0000
FOR Y =  .10    AND     N = 17 X =    -.0000
FOR Y =  .10    AND     N = 18 X =    -.0000
FOR Y =  .10    AND     N = 19 X =    -.0000
FOR Y =  .10    AND     N = 20 X =    -.0000
? .25
FOR Y =  .25    AND     N =  1 X =     .2212
FOR Y =  .25    AND     N =  2 X =     .3935
FOR Y =  .25    AND     N =  3 X =     .1734
FOR Y =  .25    AND     N =  4 X =     .0803
FOR Y =  .25    AND     N =  5 X =     .0383
FOR Y =  .25    AND     N =  6 X =     .0186
FOR Y =  .25    AND     N =  7 X =     .0091
FOR Y =  .25    AND     N =  8 X =     .0045
FOR Y =  .25    AND     N =  9 X =     .0023
FOR Y =  .25    AND     N = 10 X =     .0011
FOR Y =  .25    AND     N = 11 X =     .0006
FOR Y =  .25    AND     N = 12 X =     .0003
FOR Y =  .25    AND     N = 13 X =     .0001
FOR Y =  .25    AND     N = 14 X =     .0001
FOR Y =  .25    AND     N = 15 X =     .0000
FOR Y =  .25    AND     N = 16 X =     .0000
FOR Y =  .25    AND     N = 17 X =     .0000
FOR Y =  .25    AND     N = 18 X =     .0000
FOR Y =  .25    AND     N = 19 X =    -.0000
FOR Y =  .25    AND     N = 20 X =    -.0000
```

```
? .50
FOR Y =  .50    AND    N =  1 X =    .3935
FOR Y =  .50    AND    N =  2 X =    .6321
FOR Y =  .50    AND    N =  3 X =    .4422
FOR Y =  .50    AND    N =  4 X =    .3233
FOR Y =  .50    AND    N =  5 X =    .2424
FOR Y =  .50    AND    N =  6 X =    .1847
FOR Y =  .50    AND    N =  7 X =    .1424
FOR Y =  .50    AND    N =  8 X =    .1107
FOR Y =  .50    AND    N =  9 X =    .0866
FOR Y =  .50    AND    N = 10 X =    .0681
FOR Y =  .50    AND    N = 11 X =    .0538
FOR Y =  .50    AND    N = 12 X =    .0426
FOR Y =  .50    AND    N = 13 X =    .0339
FOR Y =  .50    AND    N = 14 X =    .0270
FOR Y =  .50    AND    N = 15 X =    .0216
FOR Y =  .50    AND    N = 16 X =    .0173
FOR Y =  .50    AND    N = 17 X =    .0138
FOR Y =  .50    AND    N = 18 X =    .0111
FOR Y =  .50    AND    N = 19 X =    .0089
FOR Y =  .50    AND    N = 20 X =    .0072
? .75
FOR Y =  .75    AND    N =  1 X =    .5276
FOR Y =  .75    AND    N =  2 X =    .7769
FOR Y =  .75    AND    N =  3 X =    .6575
FOR Y =  .75    AND    N =  4 X =    .5768
FOR Y =  .75    AND    N =  5 X =    .5162
FOR Y =  .75    AND    N =  6 X =    .4679
FOR Y =  .75    AND    N =  7 X =    .4278
FOR Y =  .75    AND    N =  8 X =    .3937
FOR Y =  .75    AND    N =  9 X =    .3641
FOR Y =  .75    AND    N = 10 X =    .3380
FOR Y =  .75    AND    N = 11 X =    .3148
FOR Y =  .75    AND    N = 12 X =    .2940
FOR Y =  .75    AND    N = 13 X =    .2752
FOR Y =  .75    AND    N = 14 X =    .2580
FOR Y =  .75    AND    N = 15 X =    .2424
FOR Y =  .75    AND    N = 16 X =    .2280
FOR Y =  .75    AND    N = 17 X =    .2147
FOR Y =  .75    AND    N = 18 X =    .2024
FOR Y =  .75    AND    N = 19 X =    .1911
FOR Y =  .75    AND    N = 20 X =    .1805
```

```
? 1.0
FOR Y = 1.00     AND     N =  1 X =     .6321
FOR Y = 1.00     AND     N =  2 X =     .8647
FOR Y = 1.00     AND     N =  3 X =     .8009
FOR Y = 1.00     AND     N =  4 X =     .7619
FOR Y = 1.00     AND     N =  5 X =     .7350
FOR Y = 1.00     AND     N =  6 X =     .7149
FOR Y = 1.00     AND     N =  7 X =     .6993
FOR Y = 1.00     AND     N =  8 X =     .6866
FOR Y = 1.00     AND     N =  9 X =     .6761
FOR Y = 1.00     AND     N = 10 X =     .6672
FOR Y = 1.00     AND     N = 11 X =     .6595
FOR Y = 1.00     AND     N = 12 X =     .6528
FOR Y = 1.00     AND     N = 13 X =     .6468
FOR Y = 1.00     AND     N = 14 X =     .6415
FOR Y = 1.00     AND     N = 15 X =     .6368
FOR Y = 1.00     AND     N = 16 X =     .6325
FOR Y = 1.00     AND     N = 17 X =     .6285
FOR Y = 1.00     AND     N = 18 X =     .6249
FOR Y = 1.00     AND     N = 19 X =     .6216
FOR Y = 1.00     AND     N = 20 X =     .6186
? 1.25
FOR Y = 1.25     AND     N =  1 X =     .7135
FOR Y = 1.25     AND     N =  2 X =     .9179
FOR Y = 1.25     AND     N =  3 X =     .8883
FOR Y = 1.25     AND     N =  4 X =     .8753
FOR Y = 1.25     AND     N =  5 X =     .8697
FOR Y = 1.25     AND     N =  6 X =     .8679
FOR Y = 1.25     AND     N =  7 X =     .8683
FOR Y = 1.25     AND     N =  8 X =     .8699
FOR Y = 1.25     AND     N =  9 X =     .8722
FOR Y = 1.25     AND     N = 10 X =     .8751
FOR Y = 1.25     AND     N = 11 X =     .8782
FOR Y = 1.25     AND     N = 12 X =     .8815
FOR Y = 1.25     AND     N = 13 X =     .8849
FOR Y = 1.25     AND     N = 14 X =     .8883
FOR Y = 1.25     AND     N = 15 X =     .8918
FOR Y = 1.25     AND     N = 16 X =     .8951
FOR Y = 1.25     AND     N = 17 X =     .8985
FOR Y = 1.25     AND     N = 18 X =     .9017
FOR Y = 1.25     AND     N = 19 X =     .9049
FOR Y = 1.25     AND     N = 20 X =     .9080
```

```
? 1.50
FOR Y = 1.50     AND     N =  1 X =     .7769
FOR Y = 1.50     AND     N =  2 X =     .9502
FOR Y = 1.50     AND     N =  3 X =     .9389
FOR Y = 1.50     AND     N =  4 X =     .9380
FOR Y = 1.50     AND     N =  5 X =     .9409
FOR Y = 1.50     AND     N =  6 X =     .9450
FOR Y = 1.50     AND     N =  7 X =     .9496
FOR Y = 1.50     AND     N =  8 X =     .9542
FOR Y = 1.50     AND     N =  9 X =     .9585
FOR Y = 1.50     AND     N = 10 X =     .9626
FOR Y = 1.50     AND     N = 11 X =     .9663
FOR Y = 1.50     AND     N = 12 X =     .9696
FOR Y = 1.50     AND     N = 13 X =     .9727
FOR Y = 1.50     AND     N = 14 X =     .9755
FOR Y = 1.50     AND     N = 15 X =     .9779
FOR Y = 1.50     AND     N = 16 X =     .9802
FOR Y = 1.50     AND     N = 17 X =     .9822
FOR Y = 1.50     AND     N = 18 X =     .9840
FOR Y = 1.50     AND     N = 19 X =     .9856
FOR Y = 1.50     AND     N = 20 X =     .9871
? 1.75
FOR Y = 1.75     AND     N =  1 X =     .8262
FOR Y = 1.75     AND     N =  2 X =     .9698
FOR Y = 1.75     AND     N =  3 X =     .9672
FOR Y = 1.75     AND     N =  4 X =     .9704
FOR Y = 1.75     AND     N =  5 X =     .9747
FOR Y = 1.75     AND     N =  6 X =     .9789
FOR Y = 1.75     AND     N =  7 X =     .9826
FOR Y = 1.75     AND     N =  8 X =     .9858
FOR Y = 1.75     AND     N =  9 X =     .9884
FOR Y = 1.75     AND     N = 10 X =     .9905
FOR Y = 1.75     AND     N = 11 X =     .9923
FOR Y = 1.75     AND     N = 12 X =     .9937
FOR Y = 1.75     AND     N = 13 X =     .9949
FOR Y = 1.75     AND     N = 14 X =     .9959
FOR Y = 1.75     AND     N = 15 X =     .9966
FOR Y = 1.75     AND     N = 16 X =     .9973
FOR Y = 1.75     AND     N = 17 X =     .9978
FOR Y = 1.75     AND     N = 18 X =     .9982
FOR Y = 1.75     AND     N = 19 X =     .9985
FOR Y = 1.75     AND     N = 20 X =     .9988
```

```
? 2.0
FOR Y = 2.00     AND     N =  1 X =     .8647
FOR Y = 2.00     AND     N =  2 X =     .9817
FOR Y = 2.00     AND     N =  3 X =     .9826
FOR Y = 2.00     AND     N =  4 X =     .9862
FOR Y = 2.00     AND     N =  5 X =     .9897
FOR Y = 2.00     AND     N =  6 X =     .9924
FOR Y = 2.00     AND     N =  7 X =     .9945
FOR Y = 2.00     AND     N =  8 X =     .9960
FOR Y = 2.00     AND     N =  9 X =     .9971
FOR Y = 2.00     AND     N = 10 X =     .9979
FOR Y = 2.00     AND     N = 11 X =     .9985
FOR Y = 2.00     AND     N = 12 X =     .9989
FOR Y = 2.00     AND     N = 13 X =     .9992
FOR Y = 2.00     AND     N = 14 X =     .9994
FOR Y = 2.00     AND     N = 15 X =     .9996
FOR Y = 2.00     AND     N = 16 X =     .9997
FOR Y = 2.00     AND     N = 17 X =     .9998
FOR Y = 2.00     AND     N = 18 X =     .9998
FOR Y = 2.00     AND     N = 19 X =     .9999
FOR Y = 2.00     AND     N = 20 X =     .9999
? 2.25
FOR Y = 2.25     AND     N =  1 X =     .8946
FOR Y = 2.25     AND     N =  2 X =     .9889
FOR Y = 2.25     AND     N =  3 X =     .9909
FOR Y = 2.25     AND     N =  4 X =     .9938
FOR Y = 2.25     AND     N =  5 X =     .9959
FOR Y = 2.25     AND     N =  6 X =     .9974
FOR Y = 2.25     AND     N =  7 X =     .9983
FOR Y = 2.25     AND     N =  8 X =     .9990
FOR Y = 2.25     AND     N =  9 X =     .9993
FOR Y = 2.25     AND     N = 10 X =     .9996
FOR Y = 2.25     AND     N = 11 X =     .9997
FOR Y = 2.25     AND     N = 12 X =     .9998
FOR Y = 2.25     AND     N = 13 X =     .9999
FOR Y = 2.25     AND     N = 14 X =     .9999
FOR Y = 2.25     AND     N = 15 X =    1.0000
FOR Y = 2.25     AND     N = 16 X =    1.0000
FOR Y = 2.25     AND     N = 17 X =    1.0000
FOR Y = 2.25     AND     N = 18 X =    1.0000
FOR Y = 2.25     AND     N = 19 X =    1.0000
FOR Y = 2.25     AND     N = 20 X =    1.0000
```

```
? 2.50
FOR Y = 2.50     AND     N =  1 X =     .9179
FOR Y = 2.50     AND     N =  2 X =     .9933
FOR Y = 2.50     AND     N =  3 X =     .9953
FOR Y = 2.50     AND     N =  4 X =     .9972
FOR Y = 2.50     AND     N =  5 X =     .9984
FOR Y = 2.50     AND     N =  6 X =     .9991
FOR Y = 2.50     AND     N =  7 X =     .9995
FOR Y = 2.50     AND     N =  8 X =     .9997
FOR Y = 2.50     AND     N =  9 X =     .9999
FOR Y = 2.50     AND     N = 10 X =     .9999
FOR Y = 2.50     AND     N = 11 X =    1.0000
FOR Y = 2.50     AND     N = 12 X =    1.0000
FOR Y = 2.50     AND     N = 13 X =    1.0000
FOR Y = 2.50     AND     N = 14 X =    1.0000
FOR Y = 2.50     AND     N = 15 X =    1.0000
FOR Y = 2.50     AND     N = 16 X =    1.0000
FOR Y = 2.50     AND     N = 17 X =    1.0000
FOR Y = 2.50     AND     N = 18 X =    1.0000
FOR Y = 2.50     AND     N = 19 X =    1.0000
FOR Y = 2.50     AND     N = 20 X =    1.0000
? 2.75
FOR Y = 2.75     AND     N =  1 X =     .9361
FOR Y = 2.75     AND     N =  2 X =     .9959
FOR Y = 2.75     AND     N =  3 X =     .9976
FOR Y = 2.75     AND     N =  4 X =     .9988
FOR Y = 2.75     AND     N =  5 X =     .9994
FOR Y = 2.75     AND     N =  6 X =     .9997
FOR Y = 2.75     AND     N =  7 X =     .9999
FOR Y = 2.75     AND     N =  8 X =     .9999
FOR Y = 2.75     AND     N =  9 X =    1.0000
FOR Y = 2.75     AND     N = 10 X =    1.0000
FOR Y = 2.75     AND     N = 11 X =    1.0000
FOR Y = 2.75     AND     N = 12 X =    1.0000
FOR Y = 2.75     AND     N = 13 X =    1.0000
FOR Y = 2.75     AND     N = 14 X =    1.0000
FOR Y = 2.75     AND     N = 15 X =    1.0000
FOR Y = 2.75     AND     N = 16 X =    1.0000
FOR Y = 2.75     AND     N = 17 X =    1.0000
FOR Y = 2.75     AND     N = 18 X =    1.0000
FOR Y = 2.75     AND     N = 19 X =    1.0000
FOR Y = 2.75     AND     N = 20 X =    1.0000
```

```
? 3.00
FOR Y = 3.00     AND     N =  1 X =     .9502
FOR Y = 3.00     AND     N =  2 X =     .9975
FOR Y = 3.00     AND     N =  3 X =     .9988
FOR Y = 3.00     AND     N =  4 X =     .9995
FOR Y = 3.00     AND     N =  5 X =     .9998
FOR Y = 3.00     AND     N =  6 X =     .9999
FOR Y = 3.00     AND     N =  7 X =    1.0000
FOR Y = 3.00     AND     N =  8 X =    1.0000
FOR Y = 3.00     AND     N =  9 X =    1.0000
FOR Y = 3.00     AND     N = 10 X =    1.0000
FOR Y = 3.00     AND     N = 11 X =    1.0000
FOR Y = 3.00     AND     N = 12 X =    1.0000
FOR Y = 3.00     AND     N = 13 X =    1.0000
FOR Y = 3.00     AND     N = 14 X =    1.0000
FOR Y = 3.00     AND     N = 15 X =    1.0000
FOR Y = 3.00     AND     N = 16 X =    1.0000
FOR Y = 3.00     AND     N = 17 X =    1.0000
FOR Y = 3.00     AND     N = 18 X =    1.0000
FOR Y = 3.00     AND     N = 19 X =    1.0000
FOR Y = 3.00     AND     N = 20 X =    1.0000
? STOP

 *TERMINATED*
```

REFERENCES CITED

1. Anderson, T.S., "Analysis and Design of Tubular Reactors," AICHE Vol 18, #1, 1972.

2. Barrett, D. "Rotating Mixer Reactor for Kinetic Studies," Trans. Inst. Chem. Engrs., Vol 49, 1971.

3. Baur, J.P., Gibbs, H.L., Wadsworth, M.E., "Initial-stage Sulfuric Acid Leaching Kinetics of Chalcopyrite Using Radiochemical Techniques," U.S.B.M., RI. 7823, 1974.

4. Bautista, R.G., "Hydrometallurgy," Advances in Chemical Engineering, Academic Press, 9, 1974.

5. Beaulieu, P.L., 1976. Personal Communication. January-March 1976. Senior Chemist for the Nevada Mining Analytical Laboratory.

6. Bielfeldt, K., "Practical Experience with the Tube Digester," Paper presented at the 7th Annual Conference of Metallurgists of the Canadian Institute of Mining and Metallurgy, Vancouver, August 25-28, 1968.

7. Brown, G.G., and Associates, Unit Operations, John Wiley and Sons, Inc., New York, New York, 1950.

8. Busev, A.E., Analytical Chemistry of Molybdenum, Daniel Davey and Co., Inc., New York, 1964.

9. Cox, H., Schellinger, A.K., "An Ion Exchange Approach to Molybdic Oxide," Engineering and Mining Journal, Vol 159, No. 10, October 1958.

10. Cremer, H.W., Watkins, S.B., Chemical Engineering Practice, Vol 8, Butterworths Publishing, London, 1965.

11. Dittman, F.W., "Epitaxial Deposition of Silicon in a Barrel Reactor," Advances in Chemical Engineering, N-133, 1974, pp. 463-473.

12. Jennings, P.H., Themelis, N.J., Stratigakos, E.S., "A Continuous-Flow Reactor for the Precipitation of Tellurium," Canadian Metallurgical Quarterly, Vol 8, #3, 1974.

13. Kramers, H., Westenterp, K.R., Elements of Chemical Reactor Design and Operation, Academic Press Inc., New York, New York, 1963.

14. Levenspiel, O., Chemical Reactor Engineering, John Wiley and Sons, New York, New York, 1972.

15. McCabe, W.L., Smith, J.C., Unit Operations of Chemical Engineering, McGraw-Hill Book Company, New York, New York, 1967.

16. McKinstry, K.A., Stermole, F.J., Dunn, R.L., "An Experimental and Theoretical Study of the Transient Response of an Isothermal Tubular Reactor with Recycle," AICHE Journal, Vol 18, #1, Jan 1972.

17. Perkin-Elmer Corp., 1973, Analytical Methods for Atomic Absorption Spectrophotometry, Norwalk, Conn.

18. Smith, J.M., Chemical Engineering Kinetics, McGraw-Hill Chemical Engineering Series, New York, New York, 1970.

19. Taggart, A.F., Handbook of Mineral Dressing, John Wiley and Sons, Inc., New York, New York, 1945.

20. Vogel, A.I., 1962, A Text-Book of Quantitative Inorganic Analysis Including Elementary Instrumental Analysis. Third Edition, Wiley and Sons, Inc., New York.

21. Weast, R.C., Handbook of Chemistry and Physics, CRC Press, Cleveland, Ohio, 1975.

22. Wolf, D., White, D.H., "Experimental Study of the Residence Time Distribution in Plasticating Screw Extruders," AICHE Journal, Vol 22, #1, Jan 1976.